Axially Chiral β,β′-Bisporphyrins: Synthesis and Configurational Stability Tuned by the Central Metals

Gerhard Bringmann,*,[†] Daniel C. G. Götz,[†] Tobias A. M. Gulder,[†] Tim H. Gehrke,[†] Torsten Bruhn,[†] Thomas Kupfer,[‡] Krzysztof Radacki,[‡] Holger Braunschweig,[‡] Alexander Heckmann,[†] and Christoph Lambert[†]

Institute of Organic Chemistry and Röntgen Research Center for Complex Material Systems, University of Würzburg, Am Hubland, D-97074 Würzburg, Germany, and Institute of Inorganic Chemistry, University of Würzburg, Am Hubland, D-97074 Würzburg, Germany

Received July 17, 2008; E-mail: bringman@chemie.uni-wuerzburg.de

Abstract: In this paper, the synthesis of a new type of intrinsically chiral, directly β,β′-linked, octa-*meso*-aryl-substituted bisporphyrins is described, by using an optimized Suzuki–Miyaura coupling procedure. This strategy leads to a broad variety of such axially chiral 'superbiaryls', differing in their metalation states and substitution patterns. On the basis of an efficient route to as-yet-unknown β-boronic acid esters of various *meso*-tetraarylporphyrins (TAPs) by a two-step bromination–borylation protocol, 18 axially chiral bisporphyrin derivatives were prepared in good to excellent yields. As compared to all other directly linked dimeric porphyrin systems, the joint presence of eight bulky meso substituents and the peripheral position of the porphyrin–porphyrin linkage is unprecedented. The axial configurations and rotational barriers of the pure atropo-enantiomers were investigated by HPLC-CD experiments on a chiral phase in combination with quantum chemical CD calculations. According to the HPLC experiments and in agreement with quantum chemical calculations by applying the dispersion-corrected BLYP method, the configurational stability of the central porphyrin–porphyrin axis strongly depends on the nature of the central metals. Cyclovoltammetric studies proved the systematic influence of the meso substituents and of the metal ions on the oxidation potentials of the bisporphyrins. The novel axially chiral bis(tetrapyrrole) compounds described here are potentially useful as substrates for asymmetric catalysis, biomimetic studies on directed electron-transfer processes, for photodynamic therapy (PDT), and for chiral recognition.

Introduction

Since the structural elucidation of chlorophyll and heme by Willstätter and Fischer in the early 20th century, the interest in chlorins, porphyrins, and related tetrapyrrolic natural products has substantially grown.[1] Besides structural work, the investigation of the biosynthetic origin and the total synthesis of naturally occurring tetrapyrrolic macrocycles were 'early' major tasks in tetrapyrrole research,[2] including the brilliant synthesis of vitamin B$_{12}$ by Woodward and Eschenmoser[3] in 1973. After the development of various methods for the functionalization of natural and fully synthetic porphyrinoids,[4] the interest has concentrated on possible applications of tetrapyrrole derivatives during the past decades.[5] Today, porphyrins play an important role in modern applied organic chemistry, e.g., as metal-organic catalysts,[6] as potent substrates in boron neutron capture therapy (BNCT),[7] in photodynamic therapy (PDT),[8] in material sciences,[9] and in biomimetic solar-energy conversion.[10]

Independent from the fruitful development of tetrapyrrole chemistry, a chemical concept of fundamental importance was established in the late 1840s: the principle of chirality. Whereas the substantial influence of stereogenic centers was thus recognized by the research community long ago, the significance of chiral axes was correctly described for the first time by Christie and Kenner no earlier than 1922.[11] Meanwhile, axial chirality—like chirality originating from stereogenic centers—is known to be important for the pharmacological activity of biarylic natural products,[12] which, in turn, has triggered the development of synthetic pathways to axially chiral natural and unnatural target molecules, among them reagents, ligands, and catalysts for asymmetric synthesis.[12,13]
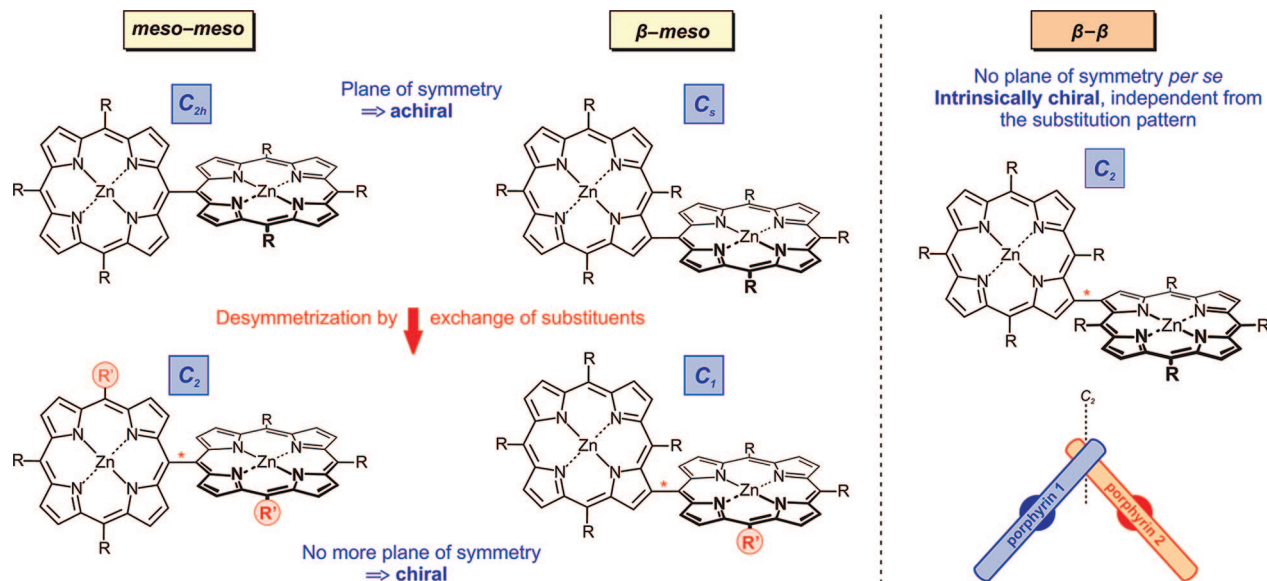
† Institute of Organic Chemistry.
‡ Institute of Inorganic Chemistry.
(1) Battersby, A. R. *Nat. Prod. Rep.* **2000**, *17*, 507–526 and references cited therein.
(2) (a) Battersby, A. R. *Nat. Prod. Rep* **1987**, *4*, 77–87 and references cited therein. (b) Battersby, A. R. *Pure Appl. Chem.* **1993**, *65*, 1113–1122 and references cited therein.

(3) (a) Woodward, R. B. *Pure Appl. Chem.* **1971**, *25*, 283–304. (b) Woodward, R. B. *Pure Appl. Chem.* **1973**, *33*, 145–177.
(4) (a) *The Porphyrin Handbook*; Kadish, K. M.; Smith, K. M., Guilard, R., Eds.; Academic Press: San Diego, 2000, Vols. *I–II*. and references cited therein. (b) *The Porphyrins*; Dolphin, D., Ed.; Academic Press: New York, 1978, Vols. *I-II* and references cited therein. (c) Shanmugathasan, S.; Edwards, C.; Boyle, R. W. *Tetrahedron* **2000**, *56*, 1025–1046 and references cited therein.
(5) *The Porphyrin Handbook*; Kadish, K. M.; Smith, K. M., Guilard, R., Eds.; Academic Press: San Diego, 2000, Vol. VI and references cited therein.
(6) (a) Fleischer, E. B.; Krishnamurthy, M. *J. Am. Chem. Soc.* **1972**, *94*, 1382–1384. (b) Ostfeld, D.; Tsutsui, M. *Acc. Chem. Res.* **1974**, *7*, 52–58. (c) Ellis, P. E.; Lyons, J. E. *Coord. Chem. Rev.* **1990**, *105*, 181–193. (d) Mansuy, D. *Coord. Chem. Rev.* **1993**, *125*, 129–142. (e) Monti, D.; Tagliatesta, P.; Mancini, G.; Boschi, T. *Angew. Chem., Int. Ed.* **1998**, *37*, 1131–1133.

Figure 1. Axial chirality in directly linked bisporphyrins: through lateral meso substituents (left) or per se, by the rather 'tangential' coupling site (right).

Still, it is only quite recently that the useful properties of porphyrins have been combined with the phenomenon of chirality.[14] The chirality of literature-known porphyrin derivatives often originates either from chiral centers or from rotationally hindered, axially chiral substituents attached to the β or meso positions.[15] Even planar-chiral porphyrin structures have been generated by unsymmetric *ansa*-like capping of the porphyrin moiety,[16] by N-methylation of a pyrrolic nitrogen starting from prochiral porphyrin derivatives,[17] or by axial coordination of the central metal, e.g., in a cobalt(III) etioporphyrin.[18]

In contrast to the structural variety represented by such common, monomeric chiral porphyrins, there are only few examples of chiral porphyrin *dimers*. For most of such optically active bisporphyrins, a spacer that links two—as such achiral—porphyrin subunits carries the chiral information.[19] Even though directly linked porphyrin complexes display a structural motif frequently used for the investigation of electron and energy transfer,[20,21] only few bisporphyrins that are based on direct meso–meso,[22,23] meso–β,[24,25] or β–β[26–29] linkages have so far been described. Only Osuka's group proved the configurational stability of three directly linked bisporphyrins, two of them being axially chiral,[30,31] one of them being doubly linked and therefore helically chiral.[21] However, all of the singly linked representatives have one—restricting—property in common: their chirality results from an unsymmetric substitution pattern, exclusively, since the basic bisporphyrin framework itself has a plane of symmetry and is therefore achiral (Figure 1). Consequently, such axially chiral dimeric porphyrins are limited to special peripheral substitution patterns that make them

unsymmetric, which moreover requires a cumbersome synthesis of their monomeric building blocks.

Dimeric porphyrins, catenated porphyrin assemblies, and multiporphyrin arrays are of growing importance,[32] i.e., because such systems possess remarkable spectral properties that are useful for electronic and optical applications.[20,21,33] Moreover, porphyrin–porphyrin (or generally, tetrapyrrole–tetrapyrrole) interactions are the basis of fundamental biological processes,[34] and thus especially of studies on 'bioinspired' electron transfer.[35] For these reasons, the synthesis of directly β,β′-linked bisporphyrins, which are intrinsically axially chiral, independent from their individual substitution pattern, and their stereochemical, spectral, and electronic characterization constitute rewarding tasks.

We herein describe a convenient, highly effective, and variable route for the synthesis of such systems and their stereoanalysis by chromatography on a chiral phase with HPLC-CD coupling, combined with quantum chemical CD calculations.[36] Key step of the synthesis is a Pd-catalyzed C—C coupling following an optimized Suzuki–Miyaura protocol.[37]

(7) (a) Barth, R. F.; Soloway, A. H.; Brugger, R. M. *Cancer Invest.* **1996**, *14*, 534–550. (b) Soloway, A. H.; Tjarks, W.; Barnum, B. A.; Rong, F.-G.; Barth, R. F.; Codogni, I. M.; Wilson, J. G. *Chem. Rev.* **1998**, *98*, 1515–1562.
(8) (a) Dougherty, T. J. *Adv. Photochem.* **1992**, *17*, 275–311. (b) Dougherty, T. J.; Marcus, S. L. *Eur. J. Cancer* **1992**, *28*, 1734–1742. (c) Bonnett, R. *Chem. Soc. Rev.* **1995**, *24*, 19–33. (d) Franck, B.; Nonn, A. *Angew. Chem., Int. Ed. Engl.* **1995**, *34*, 1795–1811. (e) Sternberg, E. D.; Dolphin, D. *Tetrahedron* **1998**, *54*, 4151–4202. (f) MacDonald, I. J.; Dougherty, T. J. *J. Porphyrins Phthalocyanines* **2001**, *5*, 105–129.

(9) (a) Adler, A. D. *J. Polym. Sci.* **1970**, *C29*, 73–79. (b) Gregg, B. A.; Fox, M. A.; Bard, A. J. *J. Phys. Chem.* **1990**, *94*, 1586–1598. (c) Lee, W.-S.; Wong, K.-Y.; Li, X.-M.; Leung, Y.-B.; Chan, C.-S.; Chan, K.-S. *J. Mater. Chem.* **1993**, *3*, 1031–1035. (d) Wagner, R. W.; Lindsey, J. S. *J. Am. Chem. Soc.* **1994**, *116*, 9759–9760. (e) Chaput, F.; Vinogradov, S. A.; Campagne, B.; Canva, M.; Boilot, J. P.; Brun, A. *Chem. Phys.* **1997**, *218*, 301–307. (f) Chen, Y.; Cao, C.; Xie, T.; Wang, X.; Lu, R.; Wang, D.; Bai, Y.; Li, T. *Supramol. Science* **1998**, *5*, 461–463. (g) Su, W.; Cooper, T. M. *Chem. Mater.* **1998**, *10*, 1212–1213. (h) Taylor, P. N.; Wylie, A. P.; Huuskonen, J.; Anderson, H. L. *Angew. Chem., Int. Ed.* **1998**, *37*, 986–989. (i) Balanda, M.; Falk, K.; Griesar, K.; Tomkowicz, Z.; Haase, W. *J. Magn. Magn. Mater.* **1999**, *205*, 14–26. (j) Burrell, A. K.; Wasielewski, M. R. *J. Porphyrins Phthalocyanines* **2000**, *4*, 401–406. (k) Falk, K.; Balanda, M.; Tomkowicz, Z.; Mascarenhas, F.; Schilling, J.; Klavins, P.; Haase, W. *Polyhedron* **2001**, *20*, 1521–1524. (l) Elemans, J. A. A. W.; van Hameren, R.; Nolte, R. J. M.; Rowan, A. E. *Adv. Mater.* **2006**, *18*, 1251–1266 and references cited therein.
(10) (a) Gust, D.; Moore, T. A. *Top. Curr. Chem.* **1991**, *159*, 103–151. (b) Gust, D.; Moore, T. A.; Moore, A. L. *Acc. Chem. Res.* **1993**, *26*, 198–205. (c) Kurreck, H.; Huber, M. *Angew. Chem., Int. Ed. Engl.* **1995**, *34*, 849–866. (d) Gust, D.; Moore, T. A.; Moore, A. L. *Acc. Chem. Res.* **2001**, *34*, 40–48.
(11) Christie, G. H.; Kenner, J. *J. Chem. Soc.* **1922**, *121*, 614–620.

Table 1. Optimization of the Reaction Conditions for the Formation of the Boronic Ester **3a**[a]
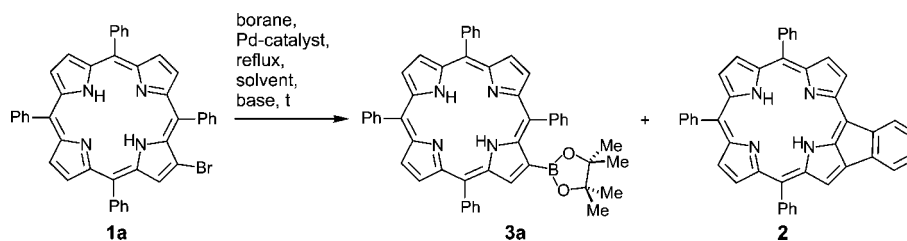
entry	solvent	additive	borane	catalyst	catalyst loading [mol %]	t [h]	hydro-debromination[b]	2 [%]	3a [%][c]
1[e]	1,2-DCE	NEt$_3$	PinBH	Pd(PPh$_3$)$_2$Cl$_2$	20	1	+	+[b]	20−30
2[f]	1,4-dioxane	KOAc	(BPin)$_2$	Pd(PtBu$_3$)$_2$	10	14	traces	−[b]	0
3	DMF	K$_2$CO$_3$	(BPin)$_2$	Pd(dppf)Cl$_2$	20	3	−	97[c]	0
4	toluene	K$_2$CO$_3$	(BPin)$_2$	Pd(dppf)Cl$_2$	20	24	+	+[b]	45−55
5	toluene	K$_2$CO$_3$	(BPin)$_2$	Pd(dppf)Cl$_2$	20	1[d]	+	+[b]	45−55
6	toluene	KOAc	(BPin)$_2$	Pd(dppf)Cl$_2$	20	12	−	−[b]	60−65
7	toluene/H$_2$O	KOAc	(BPin)$_2$	Pd(dppf)Cl$_2$	20	3	traces	−[b]	70
8	toluene/H$_2$O	KOAc	(BPin)$_2$	Pd(dppf)Cl$_2$	20	1[d]	traces	−	70
9	toluene/H$_2$O	KOAc PTC[g]	(BPin)$_2$	Pd(dppf)Cl$_2$	20	1	traces	−	67
10	toluene/H$_2$O	KOAc	(BPin)$_2$	Pd(dppf)Cl$_2$	5	46	traces	−	69

[a] Reactions were carried out under Ar with bromoporphyrin **1a** (30 mg, 1.0 equiv), bis(pinacolato)diboron (2.5 equiv), base (10 equiv), and Pd catalyst. [b] Observed by TLC. [c] Isolated yields. [d] Assisted by microwave irradiation. [e] Reaction was carried out with bromoporphyrin **1a** (30 mg, 1.0 equiv), pinacolborane (8.5 equiv), base (13 equiv), and Pd catalyst (3.0 mol %) at 90 °C as in ref 38. [f] Reaction was carried out with bromoporphyrin **1a** (30 mg, 1.0 equiv), bis(pinacolato)diboron (5.0 equiv), base (5.0 equiv), and Pd catalyst (10 mol %) as in ref 40. [g] 18-Crown-6 (10 mol %) was used as a phase-transfer catalyst.

Generating a vast chiral cavity the synthesized 'superbiaryls' should open new perspectives, e.g., as reagents, ligands, or catalysts in asymmetric synthesis. The required free-base β-boronic esters of meso-tetraaryl-substituted porphyrins (TAPs) have not yet been synthesized either.[36] Cyclic voltammetry (CV) and differential pulse voltammetry (DPV) measurements were performed to investigate the trends of oxidation potentials of all bisporphyrins depending on the type of meso substituents and metal ions. A significant result of the work is the discovery that the rotational barriers of the bisporphyrins can be tuned by the choice of the central metals.

Results and Discussion

Synthesis of β-Borylated TAPs. The scheduled construction of such bisporphyrins required the availability of β-boronic acid esters of TAP derivatives. While a versatile access to meso 'Suzuki porphyrins'[38,39] had already been described, there had as yet not been any report on the synthesis of metal-free β-borylated tetraarylporphyrins. The only known protocol for the synthesis of a metalated β-boronic acid ester of TPP (with zinc as the central metal) has recently been published by Zhang et al.,[40] starting from the respective brominated precursor. In our hands, this procedure failed to give the desired β-borylated tetraarylporphyrins both when starting from metal-free (Table 1, entry 2) or zincated bromoporphyrins.

(12) Bringmann, G.; Günther, C.; Ochse, M.; Schupp, O.; Tasler, S. In *Progress in the Chemistry of Organic Natural Products*; Herz, W., Falk, H., Kirby, G. W., Moore, R. E., Eds.; Springer: Wien, 2001, Vol. 82, pp 1−249.

(13) (a) Bringmann, G.; Walter, R.; Weirich, R. *Angew. Chem., Int. Ed. Engl.* **1990**, *29*, 977−991. (b) Bringmann, G.; Menche, D. *Acc. Chem. Res.* **2001**, *34*, 615−624. (c) Bringmann, G.; Tasler, S.; Pfeiffer, R.-M. *J. Organomet. Chem.* **2002**, *661*, 49−65. (d) Bringmann, G.; Price Mortimer, A. J.; Keller, P. A.; Gresser, M. J.; Garner, J.; Breuning, M. *Angew. Chem., Int. Ed.* **2005**, *44*, 5384−5427.

(14) Asymmetric Synthesis: (a) Collman, J. P.; Zhang, X.; Lee, V. J.; Uffelman, E. S.; Brauman, J. I. *Science* **1993**, *261*, 1404−1411. (b) Gross, Z.; Ini, S. *J. Org. Chem.* **1997**, *62*, 5514−5521. (c) Rose, E.; Quelquejeu, M.; Pandian, R. P.; Lecas-Nawrocka, A.; Vilar, A.; Ricart, G.; Collman, J. P.; Wang, Z.; Straumanis, A. *Polyhedron* **2000**, *19*, 581−586. (d) Zhang, J.-L.; Zhou, H.-B.; Huang, J.-S.; Che, C.-M. *Chem. Eur. J.* **2002**, *8*, 1554−1562. (e) Ferrand, Y.; Le Maux, P.; Simonneaux, G. *Org. Lett.* **2004**, *6*, 3211−3214. (f) Zhang, R.; Yu, W.-Y.; Che, C.-M. *Tetrahedron: Asymmetry* **2005**, *16*, 3520−3526. Chiral recognition: (g) Ogoshi, H.; Mizutani, T. *Acc. Chem. Res.* **1998**, *31*, 81−89. (h) Huang, X.; Nakanishi, K.; Berova, N. *Chirality* **2000**, *12*, 237−255. (i) Simonneaux, G.; Le Maux, P. *Coord. Chem. Rev.* **2002**, *228*, 43−60.

(15) (a) Mizutani, T.; Ema, T.; Tomita, T.; Kuroda, Y.; Ogoshi, H. *J. Chem. Soc., Chem. Commun.* **1993**, 520−522. (b) Furusho, Y.; Aida, T.; Inoue, S. *J. Chem. Soc., Chem. Commun.* **1994**, 653−655. (c) Mizutani, T.; Murakami, T.; Kurahashi, T.; Ogoshi, H. *J. Org. Chem.* **1996**, *61*, 539−548. (d) Reginato, G.; Di Bari, L.; Salvadori, P.; Guilard, R. *Eur. J. Org. Chem.* **2000**, 1165−1171. (e) Chen, Y.; Gao, G.-Y.; Zhang, X. P. *Tetrahedron Lett.* **2005**, *46*, 4965−4969. (f) Caselli, A.; Gallo, E.; Ragaini, F.; Ricatto, F.; Abbiati, G.; Cenini, S. *Inorg. Chim. Acta* **2006**, *359*, 2924−2932.

(16) (a) Morgan, B.; Dolphin, D.; Jones, R. H.; Jones, T.; Einstein, F. W. B. *J. Org. Chem.* **1987**, *52*, 4628−4631. (b) Naruta, Y.; Ishihara, N.; Tani, F.; Maruyama, K. *Bull. Chem. Soc. Jpn.* **1993**, *66*, 158−166. (c) Konishi, K.; Yahara, K.; Toshishige, H.; Aida, T.; Inoue, S. A. *J. Am. Chem. Soc.* **1994**, *116*, 1337−1344. (d) Boitrel, B.; Baveux-Chambenoît, V.; Richard, P. *Eur. J. Org. Chem.* **2001**, 4213−4221. (e) Boitrel, B.; Baveux-Chambenoît, V.; Richard, P. *Helv. Chim. Acta* **2004**, *87*, 2447−2464.

(17) (a) Kubo, H.; Aida, T.; Inoue, S.; Okamoto, Y. *J. Chem. Soc., Chem. Commun.* **1988**, 1015−1017. (b) Konishi, K.; Takahata, Y.; Aida, T.; Inoue, S.; Kuroda, R. *J. Am. Chem. Soc.* **1993**, *115*, 1169−1170. (c) Ito, A.; Konishi, K.; Aida, T. *Tetrahedron Lett.* **1996**, *37*, 2585−2588.

(18) Konishi, K.; Sugino, T.; Aida, T.; Inoue, S. *J. Am. Chem. Soc.* **1991**, *113*, 6487−6491.

(19) (a) Crossley, M. J.; Hambley, T. W.; Mackay, L. G.; Andrew, C. T.; Walton, R. *J. Chem. Soc., Chem. Commun.* **1995**, 1077−1079. (b) Crossley, M. J.; Mackay, L. G.; Try, A. C. J. *J. Chem. Soc., Chem. Commun.* **1995**, 1925−1927. (c) Ema, T.; Nemugaki, S.; Tsuboi, S.; Utaka, M. *Tetrahedron Lett.* **1995**, *36*, 5905−5908. (d) Takeuchi, M.; Chin, Y.; Imada, T.; Shinkai, S. *Chem. Commun.* **1996**, 1867−1868. (e) Flores, V.; Nguyen, C. K.; Sindelar, C. A.; Vasquez, L. D.; Shachter, A. M. *Tetrahedron Lett.* **1996**, *37*, 8633−8636. (f) Liu, H.-Y.; Huang, J.-W.; Tian, X.; Jiao, X.-D.; Luo, G.-T.; Ji, L.-N. *Chem. Commun.* **1997**, 1575−1576. (g) Ema, T.; Misawa, S.; Nemugaki, S.; Sakai, T.; Utaka, M. *Chem. Lett.* **1997**, *26*, 487−488. (h) Hayashi, T.; Nonoguchi, M.; Aya, T.; Ogoshi, H. *Tetrahedron Lett.* **1997**, *38*, 1603−1606. (i) Zaoying, L.; Jianglin, L.; Cong, L.; Wei, X. *Synth. Commun.* **2000**, *30*, 917−922. (j) Hayashi, T.; Aya, T.; Nonoguchi, M.; Mizutani, T.; Hisaeda, Y.; Kitagawa, S.; Ogoshi, H. *Tetrahedron* **2002**, *58*, 2803−2811.

The Ir-catalyzed borylation procedure starting from a bromine-free porphyrin, i.e., by direct C−H activation as elaborated by Hata et al.,[41] was not applicable to the synthesis of β-borylated TAPs either, as it is known to be limited to the preparation of porphyrin boronic acid esters having a free meso position adjacent to the center of the transmetalation.[41] Reaction of brominated TPP (**1a**) under the conditions described by Deng et al., with DMF as the solvent,[27] resulted in an almost exclusive formation of the undesired Heck product[42] **2** (Table 1, entry 3), showing the necessity to establish a basically new access to the desired porphyrin derivatives bearing four meso-aryl substituents.[36] The use of toluene as a less polar solvent finally led to the formation of the desired product **3a**, which was isolated in up to 55% yield (Table 1, entries 4 and 5). Nevertheless, the purification of the boronic acid ester was still cumbersome due to the presence of undesired byproducts—the hydrodebrominated

Table 2. Synthesis of the New β-Boronic Acid Esters **3a−k** of Metalated and Nonmetalated TAPs[a]
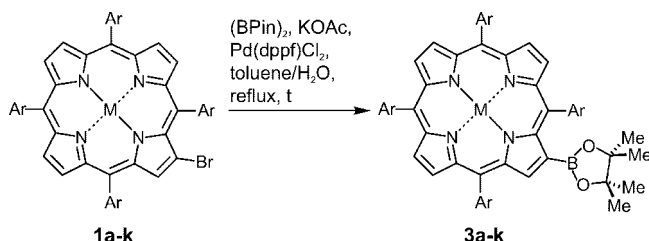
| entry	reactant	Ar	M	*t* [h]	product (yield [%])[b]
1	**1a**	phenyl	2H	3	**3a** (70)
2	**1b**	4-tolyl	2H	3	**3b** (65)
3	**1c**	4-chlorophenyl	2H	2	**3c** (56)
4	**1d**	4-methoxyphenyl	2H	3	**3d** (64)
5	**1e**	phenyl	Zn	3	**3e** (62)
6	**1f**	4-tolyl	Zn	3	**3f** (67)
7	**1g**	phenyl	Ni	3	**3g** (58)
8	**1h**	4-tolyl	Ni	3	**3h** (60)
9	**1i**	phenyl	Cu	4	**3i** (53)
10	**1j**	4-tolyl	Cu	4	**3j** (50)
11	**1k**	phenyl	Pd	4	**3k** (61)

[a] Reactions were carried out under Ar with the respective bromoporphyrin **1** (1.0 equiv), bis(pinacolato)diboron (2.5 equiv), KOAc (10 equiv), and Pd catalyst (20 mol %). [b] Isolated yields.

parent compound (TPP) and the likewise formed ring-annulated product **2**—which substantially limited the isolated yields of **3a**. Replacement of K_2CO_3 by KOAc as a more nucleophilic base increased the isolated yield up to 65% (Table 1, entry 6), presumably due to an additional activation of the boron-transferring agent by intermediate formation of a quaternary boronate anion.[43] Using toluene/H_2O as a two-phase solvent system finally led to a further improvement of the yield and to a significant reduction of the reaction time, which was again shortened by microwave irradiation or by the additional use of 18-crown-6 as a phase-transfer catalyst (Table 1, entries 5, 7, 8, and 9).[44] The borylation also succeeded by using a far smaller catalyst loading of 5 mol % (Table 1, entry 10), giving identical yields but requiring significantly extended reaction times.

Using these optimized Pd-catalyzed transmetalation conditions, several as-yet-unknown air- and water-stable porphyrin boronic acid esters **3a−k** were synthesized from the respective β-brominated tetraarylporphyrins **1a−k** in good yields and short reaction times (Table 2). Electron-withdrawing chlorine substituents (Table 2, entry 3) facilitated the competing hydrodebromination at the catalytic Pd center, presumably by an oxidative addition of hydridic boron species, followed by transmetalation and reductive elimination.[45] This would explain the slightly decreased yields as compared to the other substrates

(20) (a) Kim, D.; Osuka, A. *Acc. Chem. Res.* **2004**, *37*, 735–745. (b) Ikeue, T.; Furukawa, K.; Hata, H.; Aratani, N.; Shinokubo, H.; Kato, T.; Osuka, A. *Angew. Chem., Int. Ed.* **2005**, *44*, 6899–6901. (c) Ahn, T. K.; Kim, K. S.; Kim, D. Y.; Noh, S. B.; Aratani, N.; Ikeda, C.; Osuka, A.; Kim, D. *J. Am. Chem. Soc.* **2006**, *128*, 1700–1704.

(21) Tsuda, A.; Furuta, H.; Osuka, A. *J. Am. Chem. Soc.* **2001**, *123*, 10304–10321.

(22) (a) Susumu, K.; Shimidzu, T.; Tanaka, K.; Segawa, H. *Tetrahedron Lett.* **1996**, *37*, 8399–8402. (b) Osuka, A.; Shimidzu, H. *Angew. Chem., Int. Ed. Engl.* **1997**, *36*, 135–137. (c) Senge, M. O.; Feng, X. *Tetrahedron Lett.* **1999**, *40*, 4165–4168. (d) Senge, M. O.; Feng, X. *J. Chem. Soc., Perkin Trans. 1* **2000**, 3615–3621. (e) Aratani, N.; Osuka, A. *Org. Lett.* **2001**, *3*, 4213–4216. (f) Hiroto, S.; Osuka, A. *J. Org. Chem.* **2005**, *70*, 4054–4058. (g) Jin, L.-M.; Chen, L.; Yin, J.-J.; Guo, C.-C.; Chen, Q.-Y. *Eur. J. Org. Chem.* **2005**, 3994–4001.

(23) Khoury, R. C.; Jaquinod, L.; Smith, K. M. *Chem. Commun.* **1997**, 1057–1058.

(24) Senge, M. O.; Rößler, B.; von Gersdorff, J.; Schäfer, A.; Kurreck, H. *Tetrahedron Lett.* **2004**, *45*, 3363–3367.

(25) Ogawa, T.; Nishimoto, Y.; Yoshida, N.; Ono, N.; Osuka, A. *Angew. Chem., Int. Ed.* **1999**, *38*, 176–179.

(26) For β,β′-bisporphyrins without meso substituents that might be axially chiral but have not been stereochemically characterized, see refs 27 and 28.

(27) Deng, Y.; Chang, C. K.; Nocera, D. G. *Angew. Chem., Int. Ed.* **2000**, *39*, 1066–1068.

(28) (a) Paine III, J. B.; Dolphin, D. *Can. J. Chem.* **1978**, *56*, 1710–1712. (b) Uno, H.; Kitawaki, Y.; Ono, N. *Chem. Commun.* **2002**, 116–117.

(29) For a directly β,β′-linked, yet N-confused bisporphyrin, which has been stereochemically characterized more recently, see: (a) Siczek, M.; Chmielewski, P. J. *Angew. Chem., Int. Ed.* **2007**, *46*, 7432–7436. For its synthesis, see: (b) Chmielewski, P. J. *Angew. Chem., Int. Ed.* **2004**, *43*, 5655–5658.

(30) Nakamura, Y.; Hwang, I.; Aratani, N.; Ahn, T. K.; Ko, D. M.; Takagi, A.; Kawai, T.; Matsumoto, T.; Kim, D.; Osuka, A. *J. Am. Chem. Soc.* **2005**, *127*, 236–246.

(31) Yoshida, N.; Osuka, A. *Tetrahedron Lett.* **2000**, *41*, 9287–9291.

(32) (a) Vicente, M. G. H.; Jaquinod, L.; Smith, K. M. *Chem. Commun.* **1999**, 1771–1782. (b) Burrell, A. K.; Officer, D. L.; Plieger, P. G.; Reid, D. C. W. *Chem. Rev.* **2001**, *101*, 2751–2796.

(33) Pescitelli, G.; Gabriel, S.; Wang, Y.; Fleischhauer, J.; Woody, R. W.; Berova, N. *J. Am. Chem. Soc.* **2003**, *125*, 7613–7628.

(34) (a) van Amerongen, H.; Valkunas, L.; van Grondelle, R. *Photosynthetic Excitons*; World Scientific: Singapore, New Jersey, London, Hong Kong, 2000. (b) Blankenship, R. E. *Molecular Mechanisms of Photosynthesis*; Blackwell Science: Oxford, 2002.

(35) For recent reviews on artificial photosynthetic model systems derived from porphyrins, see: (a) Guldi, D. M. *Chem. Soc. Rev.* **2002**, *31*, 22–36. (b) Kobuke, Y.; Ogawa, K. *Bull. Chem. Soc. Jpn.* **2003**, *76*, 689–708. (c) Imahori, H. *J. Phys. Chem. B* **2004**, *108*, 6130–6143. (d) Fukuzumi, S. *Bull. Chem. Soc. Jpn.* **2006**, *79*, 177–195. (e) Satake, A.; Kobuke, Y. *Org. Biomol. Chem.* **2007**, *5*, 1679–1691. (f) Hori, T.; Nakamura, Y.; Aratani, N.; Osuka, A. *J. Organomet. Chem.* **2007**, *692*, 148–155.

(36) For preliminary results on two first representatives, see: Bringmann, G.; Rüdenauer, S.; Götz, D. C. G.; Gulder, T. A. M.; Reichert, M. *Org. Lett.* **2006**, *8*, 4743–4746.

(37) (a) Miyaura, N.; Suzuki, A. *Chem. Rev.* **1995**, *95*, 2457–2483. (b) Suzuki, A. *Proc. Jpn. Acad.* **2004**, *80*, 359–371.

(38) Hyslop, A. G.; Kellet, M. A.; Iovine, P. M.; Therien, M. J. *J. Am. Chem. Soc.* **1998**, *120*, 12676–12677. (a) In our hands these conditions published for the synthesis of *meso*-boronic acid esters of TAPs by Hyslop et al. did give β-borylated TAPs starting from the respective β-brominated porphyrins, too, but in very low yields (e.g., 25–30% for **3a** as compared to 70% with our optimized procedure, Table 1, entries 1 and 8).

(39) For some recent synthetic applications of this procedure,[38] see: (a) Tsuda, A.; Nakamura, T.; Sakamoto, S.; Yamaguchi, K.; Osuka, A. *Angew. Chem., Int. Ed.* **2002**, *41*, 2817–2820. (b) Kang, Y. K.; Rubtsov, I. V.; Iovine, P. M.; Chen, J.; Therien, M. J. *J. Am. Chem. Soc.* **2002**, *124*, 8275–8279. (c) Chng, L. L.; Chang, C. J.; Nocera, D. G. *J. Org. Chem.* **2003**, *68*, 4075–4078. (d) Cheng, F.; Zhang, S.; Adronov, A.; Echegoyen, L.; Diederich, F. *Chem. Eur. J.* **2006**, *12*, 6062–6070.

(40) Zhang, C.; Suslick, K. S. *J. Porphyrins Phthalocyanines* **2005**, *9*, 659–666.
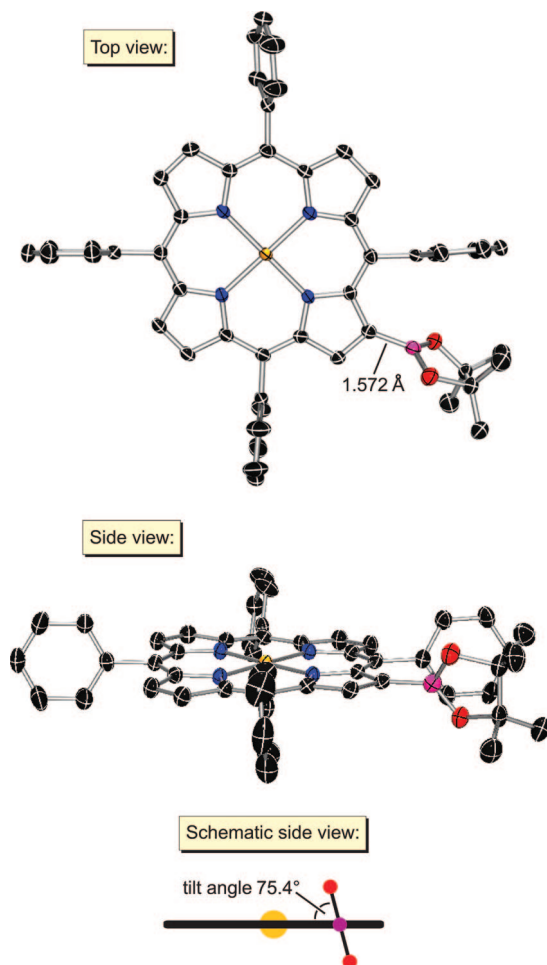
Figure 2. Molecular structure (X-ray) of {2-(4′,4′,5′,5′-tetramethyl-[1′,3′,2′]dioxaborolan-2′-yl)-5,10,15,20-tetraphenylporphyrinato}-copper(II) **3i**. Hydrogen atoms and solvent molecules (benzene) have been omitted for clarity. The thermal ellipsoids are shown at 50% probability.

bearing less electron-poor substituents on the meso-aryl residues. The influence of the central metal ion was found to be small in the case of the zinc(II), nickel(II), and palladium(II) derivatives **1e**−**1h** and **1k**, (Table 2, entries 5−8), while borylation of the brominated copper(II) porphyrins **1i** and **1j** led to significantly reduced yields (Table 2, entries 9 and 10).

The structure of the β-borylated porphyrins thus synthesized was verified by an X-ray diffraction analysis of **3i**, using crystals obtained by slow evaporation of a saturated solution in benzene (Figure 2): introduction of the boryl group in the β-position did not result in any distortion of the entirely flat porphyrin macrocycle. In contrast to previously described β-borylated porphyrins with a coplanar arrangement of the porphyrin core and the boronic acid ester unit,[41] the dioxaborolane ring is significantly tilted relative to the planar backbone by 75.4°. Similar to the structure of a meso-boryl porphyrin (torsion angle 52.0°) published by Hyslop et al.,[38] steric interactions with the adjacent meso-phenyl groups prevent the electronically favored coplanar orientation. The observed B−C bond length of 1.572 Å is in accordance with data previously published for meso- (1.57 Å)[38] and β-borylated (1.544−1.555 Å)[41] porphyrins.

In conclusion, an efficient and variable route to new β-boronic acid esters of metalated and nonmetalated tetraarylporphyrins was established, simultaneously preventing the competitive cyclization by intramolecular Heck reaction. The porphyrin derivatives thus obtained are not only of importance for the synthesis of directly β,β'-linked bisporphyrins (see below), but are also promising precursors to a broad variety of β-derivatized tetraarylporphyrins[46] and building blocks for the design of supramolecular porphyrin assemblies.[32]

Synthesis of β,β'-Linked Bisporphyrins. As reported earlier,[36] we have recently achieved the first synthetic access to intrinsically axially chiral, directly β,β'-linked bisporphyrins—a novel class of 'superbiaryls'—by a Suzuki-type cross-coupling reaction. Encouraged by these results, our efforts focused on the development of a convenient method for the synthesis of a broad range of such porphyrin-derived extended heterobiaryls, differing in their substitution patterns and metalation states (Table 3). To minimize the occurrence of reduced yields caused by the above-mentioned intramolecular Heck coupling and hydrodebromination reactions, polar solvents were initially avoided. While first attempts to achieve the coupling to generate bis-TAPs using K_3PO_4 as the base succeeded for the meso-phenyl-substituted derivative *rac*-**4a**,[36] these conditions failed to deliver the tolyl substituted product *rac*-**4b** (Table 3, entry 1). Neither microwave irradiation nor the use of KF as an additive effected a sufficient activation of the coupling partners (Table 3, entries 2 and 3). Optimum conditions in favor of the intermolecular coupling as compared to the undesired side reactions were finally found by activating the boron organyl as its more nucleophilic *at*-complex using $Ba(OH)_2 \cdot 8H_2O$ as a stronger additive (Table 3, entry 5).[37,47]

As in the case of the formation of the boronic acid esters (see above), the use of toluene/H_2O as the solvent system led to a substantially reduced reaction time and, in addition, permitted to work with a significantly smaller excess of brominated starting material **1b** (Table 3, entry 5), apparently by further increasing the concentration of $Ba(OH)_2 \cdot 8H_2O$ in the reaction system. These improvements thus provided an efficient method for the synthesis of various β,β'-linked bisporphyrins on a 300-mg scale in good, perfectly reproducible yields (Table 4).

The influence of the metalation states of the coupling partners on the reaction course was most different, depending on the respective metal: While in the case of the zinc(II) derivative, *rac*-**4f**, the yield was comparable to that of the metal-free analogue *rac*-**4a** (Table 4, entry 6), the use of the nickel(II) porphyrin boronic acid esters **3g** and **3h** led to decreased yields in the coupling step (Table 4, entries 7 and 8). The reaction of the borylated copper(II) porphyrin **3i** with the palladium(II) derivative **1k** finally resulted in significantly lower yields due to extensive hydrodebromination and hydrodeborylation (Table 4, entry 9).

(41) (a) Hata, H.; Shinokubo, H.; Osuka, A. *J. Am. Chem. Soc.* **2005**, *127*, 8264–8265. For a recent review on the regioselective borylation of porphyrins by C−H activation, see: (b) Hata, H.; Yamaguchi, S.; Mori, G.; Nakazono, S.; Katoh, T.; Takatsu, K.; Hiroto, S.; Shinokubo, H.; Osuka, A. *Chem. Asian J.* **2007**, *2*, 849–859.

(42) In the bisporphyrin synthesis by Deng et al.,[27] the monomeric coupling partners had no meso substituents, so that no competing intramolecular Heck-like cyclization could occur.

(43) Using KOAc not even traces of the Heck-annulated product **2** were detected by TLC.

(44) Kappe, C. O. *Angew. Chem., Int. Ed.* **2004**, *43*, 6250–6284.

(45) For similar results, see: Murata, M.; Watanabe, S.; Masuda, Y. *J. Org. Chem.* **1997**, *62*, 6458–6459.

(46) For similar derivatization of porphyrins without *meso*-substituents starting from the respective β-boronic acid esters, see, e.g., Deng et al.[27]

(47) Suzuki, A. *Pure Appl. Chem.* **1994**, *66*, 213–222.

Table 3. Optimization of the Coupling Conditions of **1b** and **3b** To Form the β,β′-Bisporphyrin *rac*-**4b**[a]
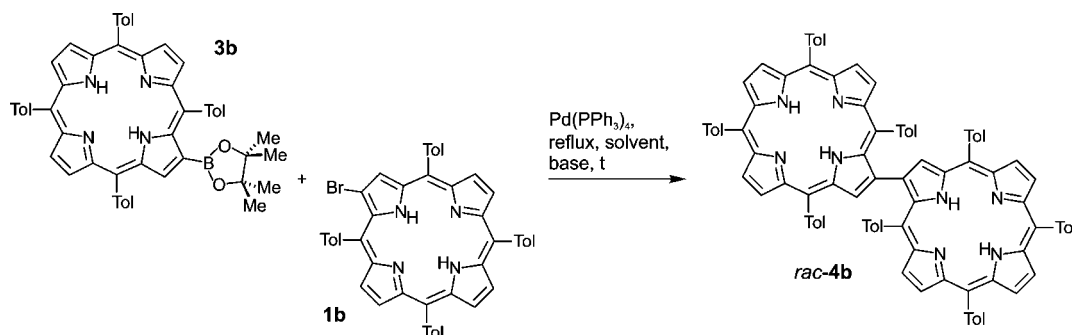
entry	solvent	base	t [h]	equiv of **1b**	hydro-debromination[b]	Heck reaction[c]	*rac*-**4b** [%][c]
1	toluene	K₃PO₄	15	4	+	+	0
2	toluene	K₃PO₄	1[d]	4	+	+	0
3	toluene	K₃PO₄/KF	15	4	+	+	traces
4	toluene	Ba(OH)₂	24	4	traces	traces	51
5	toluene/H₂O	Ba(OH)₂	14	1.2	traces	traces	71

[a] Reactions were carried out under Ar with porphyrin boronic acid ester **3b** (30 mg, 1.0 equiv), base (10 equiv), and Pd catalyst (20 mol %). [b] Observed by TLC. [c] Isolated yields. [d] Assisted by microwave irradiation.

Table 4. Synthesis of Directly β,β′-Linked Bisporphyrins[a]
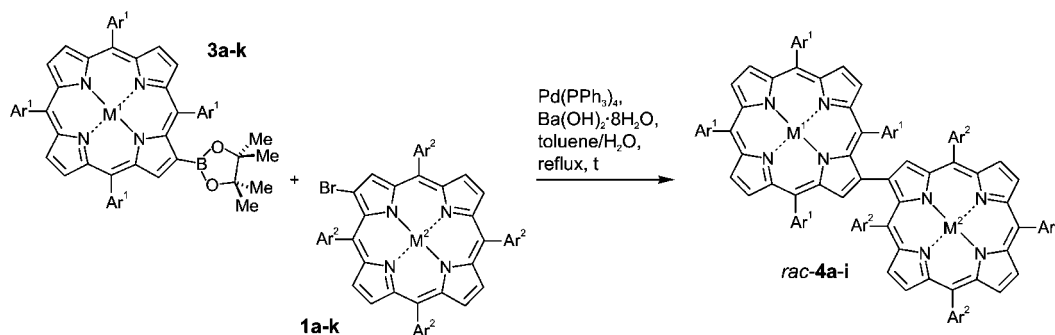
entry	reactant	Ar¹	M¹	reactant	Ar²	M²	t [h]	product (yield [%])[b]
1	**1a**	phenyl	2H	**3a**	phenyl	2H	14	*rac*-**4a** (73)
2	**1b**	4-tolyl	2H	**3b**	4-tolyl	2H	14	*rac*-**4b** (71)
3	**1c**	4-chlorophenyl	2H	**3c**	4-chlorophenyl	2H	40	*rac*-**4c** (70)
4	**1d**	4-methoxyphenyl	2H	**3d**	4-methoxyphenyl	2H	18	*rac*-**4d** (65)
5	**1b**	4-tolyl	2H	**3a**	phenyl	2H	17	*rac*-**4e** (80)
6	**1b**	4-tolyl	2H	**3f**	4-tolyl	Zn	18	*rac*-**4f** (73)
7	**1e**	phenyl	Zn	**3g**	phenyl	Ni	15	*rac*-**4g** (58)
8	**1f**	4-tolyl	Zn	**3h**	4-tolyl	Ni	16	*rac*-**4h** (50)
9	**1k**	phenyl	Pd	**3i**	phenyl	Cu	2	*rac*-**4i** (33)

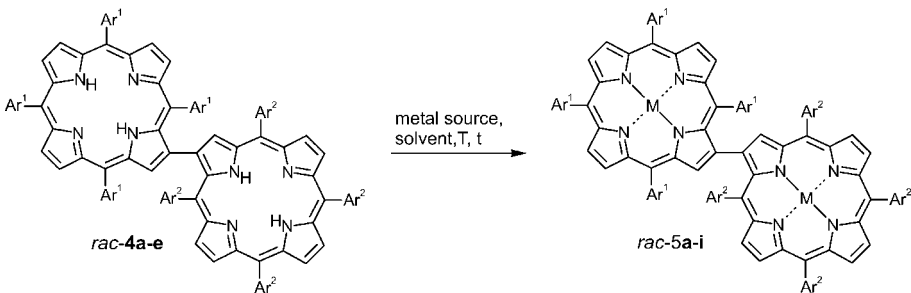[a] Reactions were carried out under Ar with porphyrin boronic acid ester **3** (1.0 equiv), bromoporphyrin **1** (1.2 equiv), Ba(OH)₂·8H₂O (10 equiv), and Pd catalyst (20 mol %). [b] Isolated yields.

An advantage of the chosen synthetic strategy is that it permits access not only to the C_2-symmetric bisporphyrins *rac*-**4a**−**d**, but, for the first time, also to the constitutionally unsymmetric representatives *rac*-**4e**−**i**. The decreased symmetry of *rac*-**4e** results from the different substitution patterns in the two monomeric porphyrin subunits, whereas in the cases of *rac*-**4f**−**i** it is the consequence of the presence of only one metal center or the combination of two different metals in the two porphyrin portions. Subsequent metalation of the free-base bisporphyrins *rac*-**4a**−**e** by literature-known procedures for the metalation of monomeric porphyrins[48] was achieved in good to excellent yields (Table 5). The corresponding nickel insertion into the monozincated derivative *rac*-**4f**, however, resulted in a scrambling of the metal centers even under mild conditions, leading to a mixture of homo- and heterogeneously bismetalated products.[49] Still, the elaborated synthetic procedure permits

generation of a broad structural diversity of these and related bisporphyrin systems.

Structure of the Bisporphyrins. Earlier optimizations of the bisporphyrin *rac*-**4a** with semiempirical (AM1) methods and of *rac*-**4a** and *rac*-**5a** with density functional calculations (B3LYP/3-21G) had yielded structures with an angle of nearly 90° between the two porphyrin planes and with an unexpectedly large distance between the phenyl substituents next to the central axis and the porphyrin subunits.[36] This was surprising at first sight because one would have supposed a larger Coulomb interaction, but in view of the fact that normal DFT methods cannot take into account such interactions, this seemed understandable. Thus, the dispersion correction introduced by Grimme,[50] which considers Coulomb interactions at a semiempirical level, was now used together with the BLYP functional and SVP[51] as the basis set for C, N, and H, and TZVP[52] for the

Table 5. Full Metalation of Directly β,β'-Linked Bisporphyrins[a]

entry	reactant	metal source	solvent	T [°C]	t [h]	M	product (yield [%])[b]
1	*rac*-**4a**	ZnCl₂	DMF	130	2	Zn	*rac*-**5a** (96)
2	*rac*-**4b**	ZnCl₂	DMF	130	2	Zn	*rac*-**5b** (98)
3	*rac*-**4c**	ZnCl₂	DMF	130	2	Zn	*rac*-**5c** (90)
4	*rac*-**4d**	ZnCl₂	DMF	130	2	Zn	*rac*-**5d** (89)
5	*rac*-**4e**	ZnCl₂	DMF	130	2	Zn	*rac*-**5e** (80)
7	*rac*-**4a**	Cu(OAc)₂	CHCl₃	62	0.5	Cu	*rac*-**5f** (78)
8	*rac*-**4a**	Ni(acac)₂	1,2-DCE	84	16	Ni	*rac*-**5g** (78)
9	*rac*-**4b**	Ni(acac)₂	1,2-DCE	84	18	Ni	*rac*-**5h** (93)
10	*rac*-**4a**	PdCl₂	benzonitrile	191	2	Pd	*rac*-**5i** (90)

[a] Reactions were carried out with β,β'-bisporphyrin *rac*-**4** (1.0 equiv) and the respective metal salt (20 equiv). [b] Isolated yields.
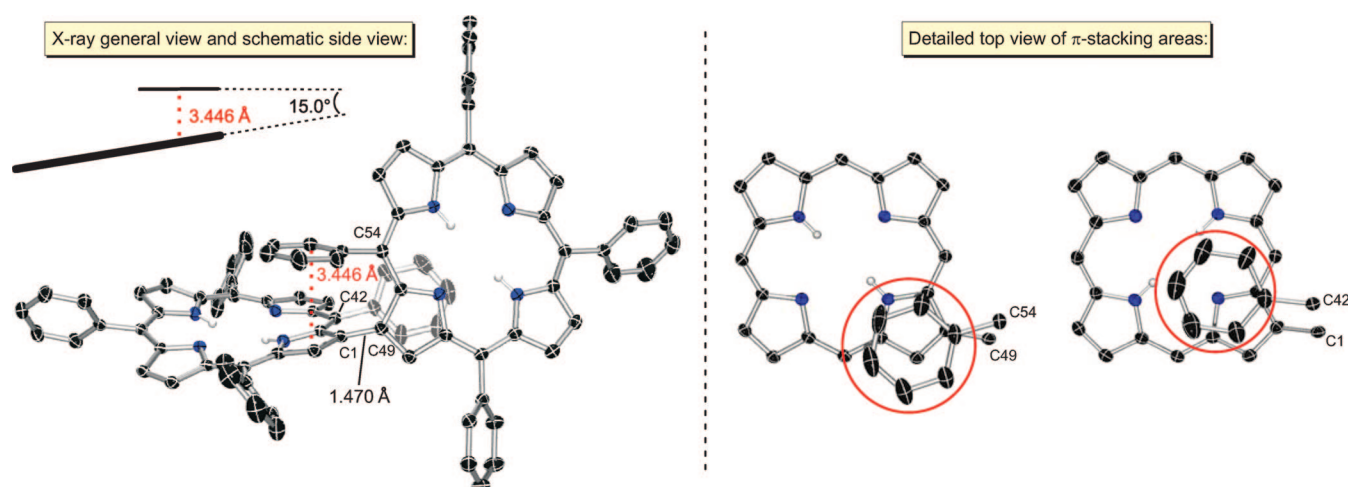

Figure 3. Molecular structure (X-ray) of β,β'-bis(5,10,15,20-tetraphenylporphyrin) *rac*-**4a** (left; hydrogen atoms and solvent molecules have been omitted for clarity) and detailed top view of possible π-stacking interactions (right; hydrogen atoms, meso phenyl groups and the second porphyrin moiety omitted). The ellipsoids are shown at 50% probability. Of the two atropo-enantiomers present in the crystal, arbitrarily only the *P* isomer is shown.

metal centers to further optimize the structures of the bisporphyrins *rac*-**4a**, *rac*-**4g**, *rac*-**5a**, *rac*-**5f**, *rac*-**5g**, and *rac*-**5i**, giving structures with a clear π-stacking between the phenyl rings at C54 and C42 and the porphyrin planes. These interactions were approved by subsequent X-ray diffraction studies of one of the racemic bisporphyrins, *rac*-**4a** (see below), yielding nearly the same structure as the calculated one.

Crystals of *rac*-**4a** suitable for this X-ray diffraction analysis were obtained by slow diffusion of *n*-hexane into a saturated solution of the compound in dichloromethane. The bisporphyrin crystallized as violet plates in a racemic form, in the triclinic space group $P\bar{1}$. The monomeric porphyrin subunits were found to be no longer planar as observed for the parent compound TPP,[53] but showed a substantially distorted saddle-shape geometry, which might be explained by disfavored steric interactions of the bulky meso substituents in the two porphyrin moieties (Figure 3). Furthermore, the bent structure facilitates intramolecular π-stacking of the meso phenyl rings next to the chiral axis and the central pyrrolic subunits linked by the porphyrin–porphyrin bond: the intercentroid distance of 3.446 Å

(48) For the insertion of zinc(II), see: (a) Adler, A. D.; Longo, F. R. *J. Inorg. Nucl. Chem.* **1970**, *32*, 2443–2445. For the insertion of nickel(II), see: (b) Annoni, E.; Pizzotti, M.; Ugo, R.; Quici, S.; Morotti, T.; Bruschi, M.; Mussini, P. *Eur. J. Inorg. Chem.* **2005**, 3857–3874. For the insertion of copper(II), see: (c) Hosseini, A.; Taylor, S.; Accorsi, G.; Armaroli, N.; Reed, C. A.; Boyd, P. D. W. *J. Am. Chem. Soc.* **2006**, *128*, 15903–15913. For the insertion of palladium(II), see: (d) Finikova, O. S.; Cheprakov, A. V.; Vinogradov, S. A. *J. Org. Chem.* **2005**, *70*, 9562–9572.

(49) As an example, reaction of *rac*-**4f** with Ni(OAc)₂·4H₂O (10 equiv) in CHCl₃/MeOH at room temperature resulted in a mixture of bisporphyrins bearing either two nickel(II), two zinc(II), or two different metal centers.

(50) Grimme, S. *J. Comput. Chem.* **2006**, *27*, 1787–1799.

(51) Schäfer, A.; Horn, H.; Ahlrichs, R. *J. Chem. Phys.* **1992**, *97*, 2571–7.
(52) Schäfer, A.; Huber, C.; Ahlrichs, R. *J. Chem. Phys.* **1994**, *100*, 5829–35.
(53) (a) Fleischer, E. B. *Acc. Chem. Res.* **1970**, *3*, 105–112. (b) Kano, K.; Fukuda, K.; Wakami, H.; Nishiyabu, R.; Pasternack, R. F. *J. Am. Chem. Soc.* **2000**, *122*, 7494–7502.
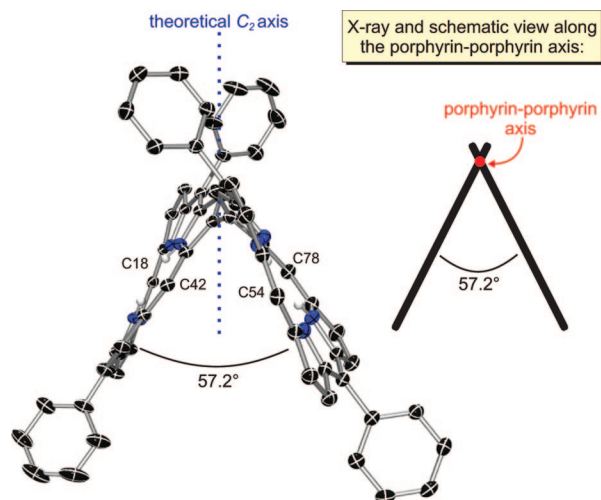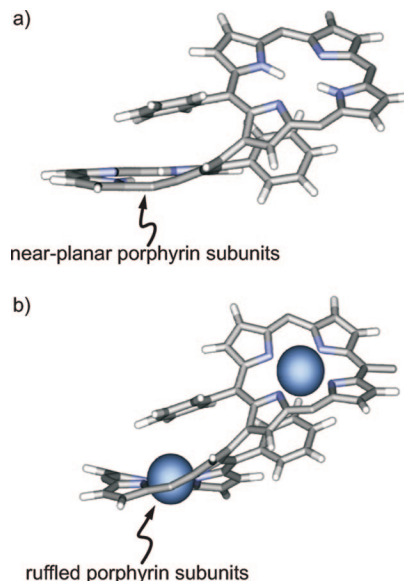
Figure 4. View along the porphyrin−porphyrin axis of **4a**: Molecular structure (X-ray, left; hydrogen atoms, phenyl moieties on C18, C42, C54, and C78 omitted for clarity) and schematic side view (right). The ellipsoids are shown at 50% probability.

between the two slipped ring systems is typical of such $\pi-\pi$ interactions;[54] the tilt angle of the phenyl ring relative to the porphyrin unit is 15.0°. The phenyl substituents next to the central axis (connected to C54 and C42) adopt two different orientations in relation to the respective adjacent porphyrin moiety: the phenyl ring at C54 is arranged fully above the porphyrin plane, while the other one has a more peripheral position (Figure 3). Consequently, the bisporphyrin slightly deviates from perfect C_2 symmetry in the crystal structure. The close proximity of the phenyl portions at C42 and C54 and the respective coplanar porphyrin subunit is also consistent with the significant diastereotopic differentiation of the corresponding phenyl protons, which had already hinted at a restricted rotation about the porphyrin−phenyl axis in previous NMR investigations.[36,55]

The mean planes of the porphyrin macrocycles as defined by the four N atoms of the respective monomeric substructures are not orthogonal to each other but form a torsion angle of 57.2° (Figure 4), which lies between typical values previously published for β,β'-linked (51.7°)[27] and meso,meso′-linked (65.0−84.0°)[23] bisporphyrins. If, however, one defines the dihedral angle between the two molecular portions by the mutual array of the two pyrrole rings that form the inner part of the heterobiaryl system (which has not been done for the other derivatives in the literature), the angle is much higher, viz 75.9°, thus reflecting the high degree of molecular torsion of the two porphyrin subunits.

The length of the central C1−C49 bond (1.470 Å) correlates with the respective values observed for a similar β,β'-linked bisporphyrin, yet without phenyl portions in the meso positions (1.46 Å),[27] and with those of an N-confused β,β'-bisporphyrin (1.468 Å).[29] As mentioned the directly linked pyrrole subunits are substantially tilted against each other (75.9°), which, at first sight, should be unfavorable for the electronic 'communication'

(54) Hunter, C. A.; Sanders, J. K. M. *J. Am. Chem. Soc.* **1990**, *112*, 5525–5534.

(55) For a report on the electronic influence of para substituents on the rotational barriers of the aryl residues in ruthenium, indium, and titanium complexes of *meso*-tetraarylporphyrins, see: Eaton, S. S.; Eaton, G. R. *J. Am. Chem. Soc.* **1977**, *99*, 6594–6599.

(56) *Handbook of Chemistry and Physics*, 79th ed.; Lide, D. R., Ed.; CRC Press: Boca Raton, Boston, London, New York, Washington D.C., 1998.

Figure 5. Side view of the optimized (BLYP-D/SVP, TZVP) structures a) of *rac*-**4a** (M^1/M^2 = 2H/2H) and b) *rac*-**5g** (M^1/M^2 = Ni/Ni); some of the phenyl substituents were omitted for reasons of clarity. While the free-base structure shows nearly planar porphyrin subunits, the molecular portions of the bis-metalated compound adopt a ruffled conformation.

between the two macrocycles. Nonetheless, the central C−C axes of all these β,β'-bisporphyrins ('conventional' or N-confused) are significantly shorter than typical $C_{aryl}-C_{aryl}$ bonds,[56] suggesting greater electronic interaction between the two β,β'-bridged porphyrin subunits than in the case of meso,meso′-linked bisporphyrins, which show a typical bond length of 1.51 Å.[23] The described crystal structure is unique as no X-ray diffraction analysis of a β,β'-bisporphyrin with meso-aryl substituents has so far been reported.

The calculated structures of *rac*-**4a**, *rac*-**4g**, *rac*-**5a**, *rac*-**5f**, and *rac*-**5i** look very similar to each other because in the free base and most of the metalated bisporphyrins the porphyrin subunits are close to planarity. The only exception is the metalated dimer *rac*-**5g**, where the two nickel(II) porphyrin moieties are largely distorted and have a ruffled conformation (Figure 5).

Spectral Properties. As expected, the UV spectra of all metal-free β,β'-bisporphyrins, *rac*-**4a**−**e**, showed the B band (Soret band) at about 425 nm and the four Q bands between 520 and 660 nm. As in the cases of achiral meso,meso-linked porphyrin dimers[22,23] and alkyl-substituted β,β'-bisporphyrins that have no meso substituents,[26] the interaction of the electric transition dipole moments of the single porphyrin moieties connected with each other results in an exciton coupling. As a consequence, a Davydov splitting of the B band was observed (Figure 6a), with an energy gap of about 800 cm^{-1} (energetic difference between B_1 and B_2), which is typical of β,β'-linked bisporphyrins,[27] while the meso,β- and meso,meso-coupled ones display B-band splittings of about 1300 and 2100 cm^{-1}, respectively.[25] The comparison between the UV spectrum and the CD curves of the respective atropo-enantiomers proved that the doublet of the Soret band indeed belonged to an exciton splitting, since the wavelengths of B_1 and B_2 in the former one matched the extreme values in the latter ones, while the wavelength of the relative minimum between B_1 and B_2 corresponded to the inflection points of the CD couplets (Figure 6c).
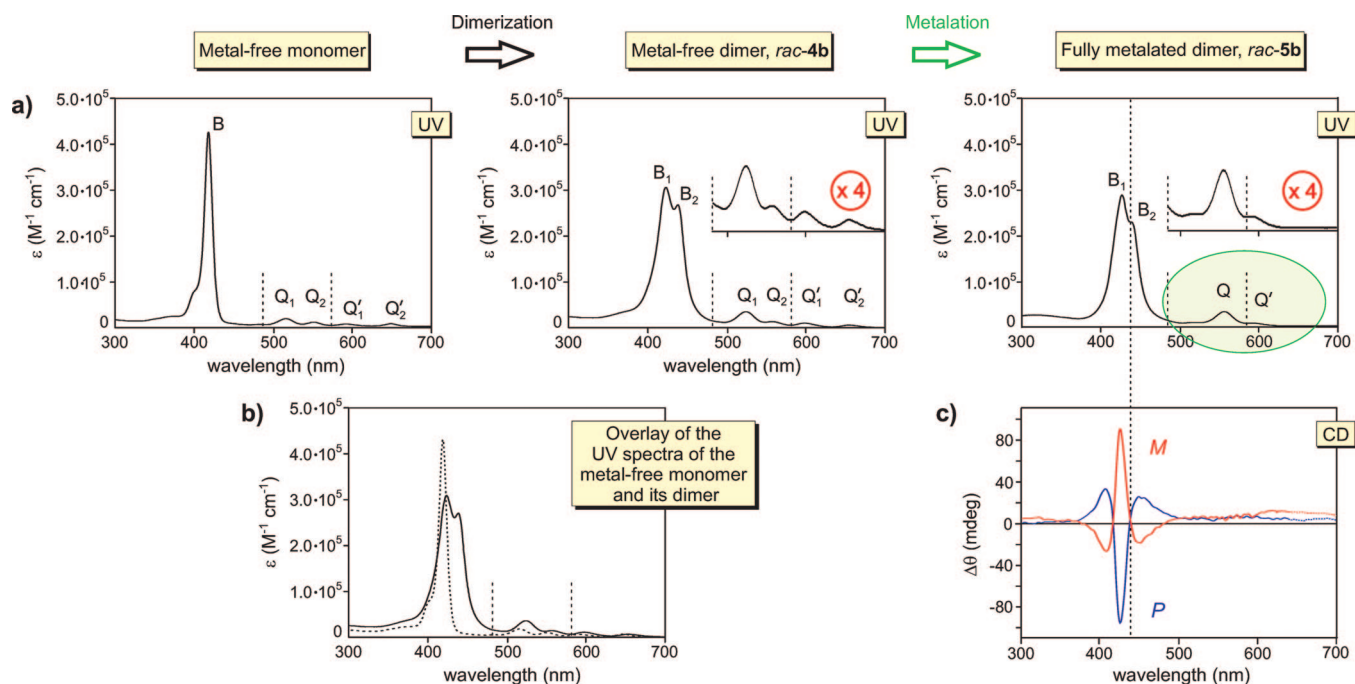
In addition, the B band appeared broadened and slightly decreased in intensity, whereas the Q bands exhibited an

Figure 6. (a) Comparison of the UV spectra of monomeric porphyrins and β,β'-bisporphyrins, exemplarily shown for the monomer 5,10,15,20-tetra(4-tolyl)porphyrin (left), its metal-free dimer, *rac*-**4b** (center), and the fully zincated derivative *rac*-**5b** (right). (b) Overlay of the UV spectra of 5,10,15,20-tetra(4-tolyl)porphyrin and *rac*-**4b**. (c) Correlation of the CD curves of the respective atropisomers of *rac*-**5b** to its UV spectrum.
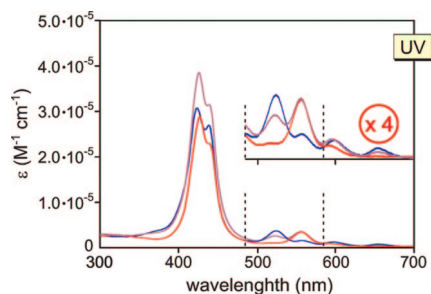
Figure 7. UV spectra of the metal-free bisporphyrin *rac*-**4b** (blue), of its monozincated derivative *rac*-**4f** (purple), and the fully metalated (two times Zn) analogue, *rac*-**5b** (red), in dichloromethane. The spectrum of the monometalated bisporphyrin *rac*-**4f** is composed of the spectrum of the metal-free bisporphyrin *rac*-**4b** and that of its fully metalated derivative, *rac*-**5b**.

increased intensity (Figure 6b). Furthermore, the entire UV spectra of β,β'-bisporphyrins were red-shifted as compared to the respective monomeric forms (Figure 6b), indicative of the occurrence of further effects, like electronic couplings[27] or charge-transfer transitions.[31]

As for monomeric porphyrins,[57] full metalation of the synthesized dimers gave rise to a higher molecular symmetry, leading to a degeneration of the transitions Q_1/Q_2 and Q_1'/Q_2' to give only two Q bands (Q and Q', respectively) for the substances *rac*-**4g**–**i** and *rac*-**5a**–**i** (Figure 6a). The UV profile of the monometalated bisporphyrin *rac*-**4f** displays the bands typical of both, the metal-free bisporphyrin (*rac*-**4b**) and the fully metalated one (*rac*-**5b**, Figure 7). A more detailed assignment of electronic transitions and dicussion of the excitonic effects in all bisporphyrins is hampered by a strong overlap of multiple B bands, which is caused by the low symmetry even of fully metalated bisporphyrins.

(57) (a) Gouterman, M. *J. Mol. Spectrosc.* **1961**, *6*, 138–163. (b) Gouterman, M. In *The Porphyrins*; Dolphin, D., Ed.; Academic Press: New York, 1978, Vol. III, pp 1–165.

Stereochemical Analysis. For stereochemical analysis, the (racemic) metalated bisporphyrins thus prepared had to be resolved into their atropo-enantiomers by HPLC on a chiral phase, which had initially, for *rac*-**5a** (and for *rac*-**5b**), succeeded by using a Chirex-3010 column (Phenomenex) at room temperature. The configuration at the biaryl axis of the enantiomers *P*-**5a** and *M*-**5a** (and of *P*- and *M*-**5b**) had been established by HPLC-CD experiments in the stopped-flow mode in combination with quantum chemical CD calculations, revealing the *P* atropo-enantiomer to be the faster one.[36] Since these earlier calculations had only been done for the free base as a simplified model compound and because the new, higher-level methods used in this paper to optimize the structure now yielded significantly more accurate structures, the CD spectrum of the bisporphyrin *rac*-**5a** was recalculated, too, and these calculations confirmed the absolute configurations attributed before (see Supporting Information).

Individual optimization of the HPLC conditions for the metalated dimers *rac*-**4g**, *rac*-**4h**, and *rac*-**5b**−**e** resulted in clear baseline separations with short retention times and perfectly mirror-shaped CD curves (recorded in the stopped-flow mode) for the respective atropo-enantiomers (Figure 8). As expected, all CD spectra were strongly related to those of **5a**, permitting configurational assignment by comparison of these curves with the ones calculated for the enantiomers of the parent dimer **5a**, *P*-**5a**, and *M*-**5a**. This clearly evidenced the chromatographically faster atropo-enantiomers of **4g**, **4h**, and **5a**−**e** to be *P*-configured, and, as a consequence, the slower ones to have the *M* configuration at the porphyrin−porphyrin axis. The palladium(II) and copper(II) bisporphyrins *rac*-**4i**, *rac*-**5f**, and *rac*-**5i**, by contrast, showed an opposite chromatographical behavior, with the *M* enantiomer being the faster eluting one. That this inversion is due to a different chromatographic behavior and not a consequence of inverted CD spectra is confirmed by satisfying accordance of the experimental CD curves of the copper(II)/copper(II) and palladium(II)/palladium(II) bispor-
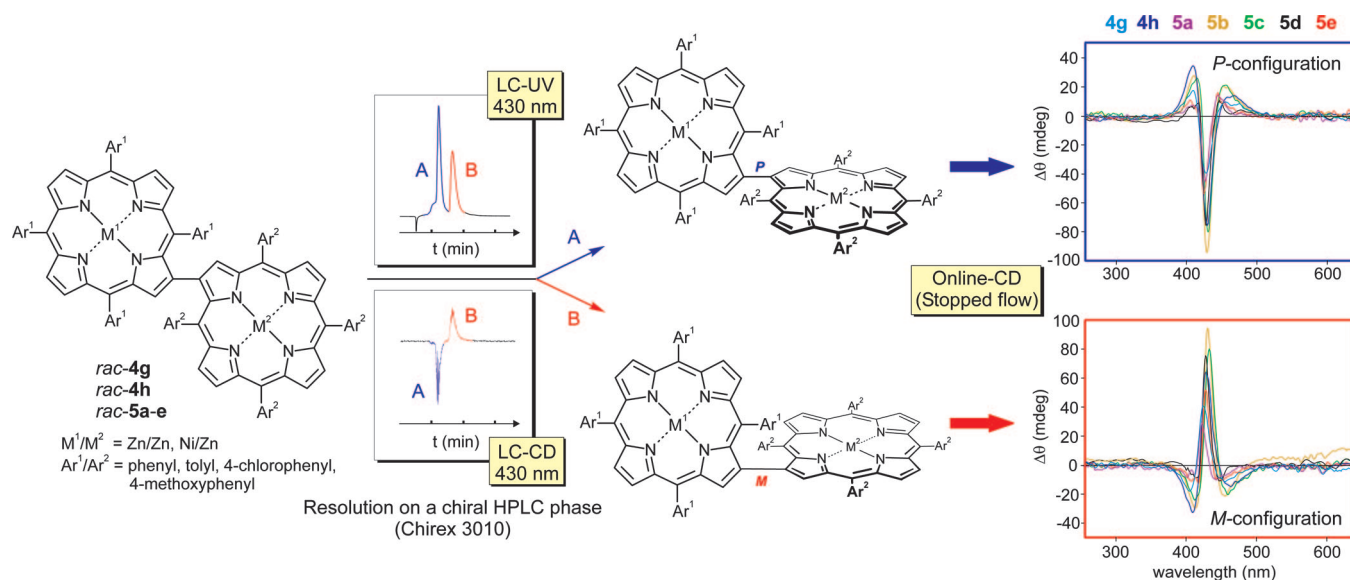
Figure 8. Stereochemical characterization of the bisporphyrins by online HPLC-CD measurements on a chiral phase, exemplarily shown for **4g**, **4h**, and **5a**–**e**.

phyrins *rac*-**5f** and *rac*-**5i** with the spectra calculated for these compounds. Moreover, the computed structures of the different bisporphyrins are very similar to each other, independent from the central metal. These findings preclude that there are metal-induced conformational changes that might lead to fully inverted CD spectra.

Although the simple exciton coupling theory is not generally applicable to optically active porphyrin dimers,[58] all of the stereochemical assignments thus achieved were in agreement with the results when applying the exciton chirality[59] approach, according to which those enantiomers of the fully metalated dimeric porphyrins that possess a positive first couplet around 450 nm should be interpreted to have a 'positive chirality', i.e., to be *P*-configured; and, vice versa the peaks with a negative couplet should correspond to the *M* enantiomers.

Configurational Stability Depending on the Central Metal Atoms. Unexpectedly, all attempts to resolve the free-base bisporphyrins *rac*-**4a**–**e**, the monometalated dimer *rac*-**4f**, or the fully metalated nickel(II) dimers *rac*-**5g** and *rac*-**5h** into their atropo-enantiomers failed, even on a variety of different chiral HPLC phases.[60] One reason for the observed chromatographic behavior could be that enantiomer-specific interactions of the bisporphyrins with the stationary phase are more differentiated in the presence of certain metal centers. Alternatively, the nature of the central metal might influence the geometry of the dimer, possibly including the configurational stability at the axis; in fact, the metal center has been reported to rigidify the molecular framework and, thus, to influence rotational barriers of attached aryl (though not porphyrin) substituents.[61] Hence, it is imaginable that the metal insertion into the porphyrin backbone might not only effect a conformational change of the macrocycle,[62] but could also increase the rotational barrier about the

porphyrin–porphyrin axis. In this case the failure to resolve the enantiomers of the metal-free, the monometalated, and the nickelated bisporphyrins might be due to their configurational instability. This hypothesis was supported by the fact that complete racemization was observed when submitting an enantiopure sample of **5a** to demetalation (room temperature, aqueous 1 N HCl) and subsequent remetalation under mildest possible conditions, which hinted at a significantly lowered rotational barrier of the generated metal-free intermediate, yet not fully excluding an acid-catalyzed racemization process. These findings made it rewarding to further investigate the metal influence on the configurational stability.

In a first set of experiments the rotational stability of the stereogenic axes of the homometalated dimers *rac*-**5a** (M^1/M^2 = Zn/Zn), *rac*-**5f** (M^1/M^2 = Cu/Cu), and *rac*-**5i** (M^1/M^2 = Pd/Pd) at room temperature was investigated using the respective *P*-configured stereoisomers: Enantiopure samples were isolated by repeated HPLC runs on a semipreparative Chirex-3010 column, stored at room temperature, and analyzed by HPLC at regular intervals (Figure 9a).

After 24 h no interconversion of *P*-**5a** into the corresponding enantiomer *M*-**5a** was observed, suggesting that the porphyrin–porphyrin axis of *P*-**5a** is rotationally fully stable at room temperature. Within the same period, the enantiomeric purity of the palladium(II) bisporphyrin *rac*-**5i** decreased to 82% ee, while the copper(II) derivative *rac*-**5f** was already almost racemic (4% ee). Thus, the barrier of the racemization process strongly depends on the central metals, decreasing in the order zinc(II)/zinc(II) > palladium(II)/palladium(II) > copper(II)/ copper(II) > nickel(II)/nickel(II) ≈ zinc(II)/free-base ≈ free-base/free-base (Figure 9a). This remarkable phenomenon—the metal influence on the rotational barrier of a porphyrin–porphyrin axis—had not previously been described in the literature. By

(58) Muranaka, A.; Asano, Y.; Tsuda, A.; Osuka, A.; Kobayashi, N. *ChemPhysChem* **2006**, *7*, 1235–1240.

(59) Harada, N.; Nkanishi, K. *Circular Dichroic Spectroscopy: Exciton Coupling in Organic Stereochemistry*; University Science Books: Mill Valley, CA, 1983.

(60) In agreement with these results, the enantiomeric resolution of previously reported axially chiral meso,meso′-linked bisporphyrins by HPLC on a chiral phase had likewise succeeded only for the fully metalated derivatives.[30]

(61) Medforth, C. J.; Haddad, R. E.; Muzzi, C. M.; Dooley, N. R.; Jaquinod, L.; Shyr, D. C.; Nurco, D. J.; Olmstead, M. M.; Smith, K. M.; Ma, J.-G.; Shelnutt, J. A. *Inorg. Chem.* **2003**, *42*, 2227–2241. For an earlier, yet more special report on phenyl ring rotation in monomeric ruthenium, indium, and titanium tetraarylporphyrins, see ref 55.

(62) (a) Scheidt, W. R.; Lee, Y. J. *Struct. Bonding (Berlin)* **1987**, *64*, 1–70. (b) Senge, M. O. *J. Photochem. Photobiol., B* **1992**, *16*, 3–36.
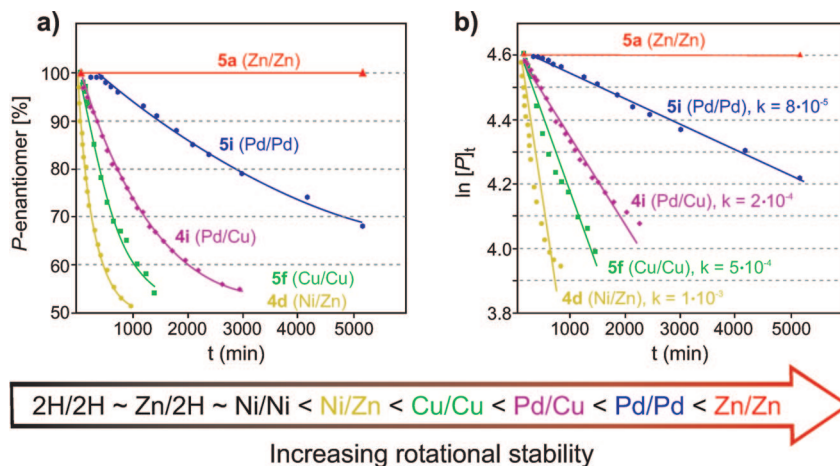
Figure 9. (a) Metal-dependence of the racemization of symmetrically (**5a**, **5i**, and **5f**) and nonsymmetrically (**4d** and **4i**) metalated dimeric porphyrins over time at room temperature. (b) Determination of rate constants at room temperature assuming a first-order kinetic. The metal-free, the monometalated, and the nickelated bisporphyrins could not be resolved due to their configurational instability.
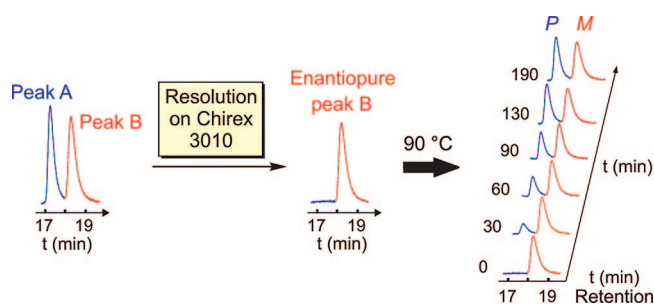
Figure 10. Experimental determination of the atropisomerization rate, exemplarily shown for *rac*-**5a**, by resolution of its two atropo-enantiomers, *P*-**5a** (peak A, blue) and *M*-**5a** (peak B, red), followed by thermal equilibration (here exemplarily shown for 90 °C) of *M*-**5a** over time in toluene, monitored by analytical HPLC on a chiral phase (Chirex 3010).

in-depth investigation of the isomerization barriers of the configurationally most stable bisporphyrin **5a** and the semistable, but still separable copper(II) derivative **5f**, the range of the energies of activation for the atropo-enantiomerization of this new class of optically active bisporphyrins was determined.

The rotational stability of the biaryl axis of the bisporphyrin **5a** was investigated more closely by HPLC-UV measurements of the temperature-dependent atropisomerization of the above prepared enantiopure material, this time exemplarily for *M*-**5a** (Figure 10). The atropo-enantiomerization was monitored at three different temperatures (90, 100, 110 °C),[63] permitting evaluation of the respective rate constants of the racemization process, and thus to calculate the Gibbs free energy of activation at room temperature (25 °C) by the Eyring equation. The experimental value thus obtained, $\Delta G_{rot}(\mathbf{5a})^{exp} = 114.9$ kJ mol^{-1}, clearly proved the rotational stability of the 2-fold zincated bisporphyrin **5a**.

The isomerization process of the copper(II) bisporphyrin **5f** was investigated analogously at 25, 40, and 62 °C, resulting in a rotational barrier of $\Delta G_{rot}(\mathbf{5f})^{exp} = 101.1$ kJ mol^{-1}. This value is thus in good agreement with the observed slow interconversion of the atropo-enantiomers at room temperature. The Gibbs free energies of activation of the chromatographically separable dimers thus range from 101.1 kJ mol^{-1} for the configurationally semistable bisporphyrin **5f** ($M^1/M^2 =$ Cu/Cu) to 114.9 kJ mol^{-1} for the fully stable derivative **5a** ($M^1/M^2 =$ Zn/Zn). The determination of these boundary values, together with the likewise experimentally measured rate constants of **5i** (M^1/M^2

$=$ Pd/Pd), and the heterogeneously metalated **4i** ($M^1/M^2 =$ Pd/Cu) and **4d** ($M^1/M^2 =$ Ni/Zn) at room temperature (Figure 8b), permitted to rank the synthesized 'superbiaryls' by their stabilities: zinc(II)/zinc(II) (114.9 kJ mol^{-1}) > palladium(II)/palladium(II) > palladium(II)/copper(II) > copper(II)/copper(II) (101.1 kJ mol^{-1}) > nickel(II)/zinc(II) > nickel(II)/nickel(II) ≈ zinc(II)/free-base ≈ free-base/free-base (not resolvable, even at 0 °C). Therefore, the decisive factor for the rotational stability might indeed be a conformational change of the porphyrin subunits due to the ion radius and/or the electronic character of the central metals. The mixed metalated bis-TAP **4i** ($M^1/M^2 =$ Pd/Cu) nicely confirms the expected tendencies, as it exhibits an energy of activation right in between the respective homo-metalated systems. The nickel(II)/zinc(II) derivative **4d**, however, suggests that the conformationally labile part of the bisporphyrins is decisive for the rotational barrier as its energy of activation is even lower than the one of the semistable copper(II)/copper(II) dimer **5f**, although it has at least one zincated porphyrin half.

Computational Studies on the Atropisomerization Process. To get deeper insight into this observed metal-dependent configurational behavior, the rotational barriers of the different bisporphyrins were calculated with the BLYP-D method and the above-mentioned combination of basis sets. Two possible transition states were found for each of the calculated bisporphyrins, of which only the energetically clearly favored ones will be discussed here. These transition states look quite similar for all bisporphyrins (except for $M^1/M^2 =$ Ni/Ni, see below), with the porphyrin planes themselves being slightly saddle-shaped distorted and nonplanar (Figure 11). The angle between the porphyrin planes varies depending on the kind of central atoms (metal or, in the case of the free base, the two hydrogens). While in previous investigations based on simpler theoretical methods, nearly no difference in the rotational barriers between zinc(II)/zinc(II) and the free base had been found,[36] the dispersion-corrected calculations now provided clear differences between the investigated bisporphyrins. Unfortunately, the calculated barriers are systematically, by about 50 kJ mol^{-1}, too high in comparison to the experimental values (Table 6)

(63) The new dimers described in this paper are configurationally not as stable as the meso,meso′-linked bisporphyrins previously reported.[31] The synthesis of β,β′-bisporphyrins with additional β-substituents next to the central axis is currently in progress in our group.
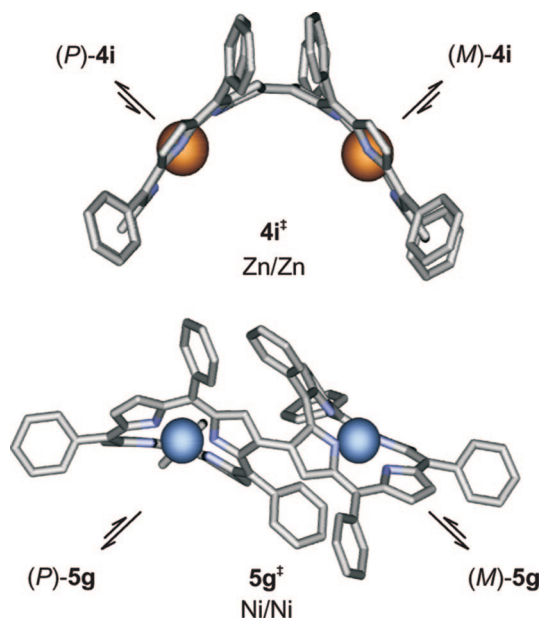
Figure 11. BLYP-D/SVP and TZVP-optimized transition states for the atropisomerization of **4i** (stereochemically stable) and **5g** (configurationally unstable). The ruffled conformation of the porphyrin subunits in **5g** yields a substantially different transition state as compared to that of **4i,** which has slightly saddle-shaped porphyrin moieties.

Table 6. Calculated (BLYP-D; SVP as a Basis Set for C, H, and N and TZVP for Metal Atoms) and Experimental Rotational Barriers of Selected Bisporphyrins[a]

	central atoms	ΔE (gas phase) [kJ mol^{-1}]	ΔG (exp.) [kJ mol^{-1}]
rac-**4a**	2H/2H	99 (94)	–
rac-**5g**	Ni/Ni	128 (129)	–
rac-**4g**	Zn/Ni	153 (149)	–[b]
rac-**5f**	Cu/Cu	156 (153)	101
rac-**5i**	Pd/Pd	156 (153)	–[b]
rac-**5a**	Zn/Zn	163 (160)	115

[a] The results of the COSMO calculations are given in parentheses. [b] Not measured.

and even calculations in a solvent field with COSMO[64] or calculations with a higher-level method, viz. the dispersion-corrected double hybrid functional B2PLYP-D,[65] exemplarily performed for the bis-zinc(II) and the bis-palladium(II) case (viz. bisporphyrins *rac*-**5a** and *rac*-**5i**), did not give significantly lower values. Nonetheless, the results confirm the experimentally determined order of stability with zinc(II)/zinc(II) (exptl 115 kJ mol^{-1}, calcd 163 kJ mol^{-1}) possessing the most stable axial configuration and with copper(II)/copper(II) (exptl 101 kJ mol^{-1}, calcd 156 kJ mol^{-1}) and zinc(II)/nickel(II) (calcd 152 kJ mol^{-1}) having the configurationally least stable arrays.[66] Keeping in mind that the energy is calculated too high (by about 50 kJ mol^{-1}), the nickel(II)/nickel(II) (calcd 128 kJ mol^{-1}) and the free-base bisporphyrins (calcd 99 kJ/mol) are configurationally unstable as also seen in the experiment.

As mentioned above, the differences in the optimized structures are small, but still large enough to explain the order

(64) Klamt, A. *COSMO-RS: From Quantum Chemistry to Fluid Phase Thermodynamics and Drug Design*; Elsevier: Amsterdam, 2005.
(65) Grimme, S. *J. Chem. Phys.* **2006**, *124*, 034108/1–034108/16.
(66) Regarding the rotational barriers the calculations fail to differentiate between the Pd/Pd and the Cu/Cu dimer, certainly because the Pd/Pd complex should be influenced by relativistic effects that can not be taken into account with the used methods.

Table 7. Redox Potentials of *rac*-**4a**−**i** and *rac*-**5a**−**i** As Determined by DPV (Scan Rate: 20 mVs^{-1}), Referenced against Fc/Fc$^+$ As the Internal Standard (0.1 M TBAH in CH$_2$Cl$_2$)

	$E_{1/2}$ (Ox1) [mV]	$E_{1/2}$ (Ox2) [mV]	$E_{1/2}$ (Ox3) [mV]	$E_{1/2}$ (Ox4) [mV]	ΔE (Ox1 − Ox2) [mV]
rac-**4a**	480	565	825[a]		85
rac-**4b**	470	550	820[a]		80
rac-**4c**		640[a]	895[a]		–
rac-**4d**		445[a]	675[a]		–
rac-**4e**	450	570	830[a]		(120)[b]
rac-**4f**	340	490	650	890	(150)[b]
rac-**4g**	390	570	690	950	(180)[b]
rac-**4h**	370	550	660	925	(180)[b]
rac-**4i**	485	720	965	1140	(235)[b]
rac-**5a**		410[a]	655[a]		–
rac-**5b**		380[a]	650[a]		–
rac-**5c**		490[a]	735[a]		–
rac-**5d**		335[a]	585[a]		–
rac-**5e**	350	415	650[a]		(65)[b]
rac-**5f**	430	535	940[a]		105
rac-**5g**	510	650	960[a]		140
rac-**5h**	455	590	925[a]		135
rac-**5i**	595	710	1100[a]		115

[a] Two-electron process not resolvable even by DPV. [b] ΔE resulting from different oxidation potentials of two different porphyrin subunits.

of configurational stability as experimentally established above. The absence of a central metal in the free base makes it easier for the porphyrin rings to attain the nonplanar arrangement as required for the transition state. Whereas in the case of zinc(II), palladium(II), and copper(II) the ground-state has planar porphyrin subunits, so that the system has to deviate from this orientation in the transition state, the porphyrin plane with nickel already shows a ground-state orientation closely related to the transition state, thus leading to a much lower rotational barrier. The results show that the rigidity of the porphyrin subunits causes the largely different barriers observed. Consequently, the better the central metal fits into the porphyrin ring and, hence, the more planar (and 'relaxed') this ring is in the ground state, the higher will be the energy required to overcome the ring strain in the transition state and, thus, the more stable is the configuration at the central axis.

In the bis-nickel system *rac*-**4i**, the porphyrin moieties are ruffled (and, possibly, more flexible due to the smaller central metal) and the transition state is clearly different from all other ones investigated so far. This divergent orientation and thus the resulting smaller steric hindrance is the reason for the much lower rotational barrier.
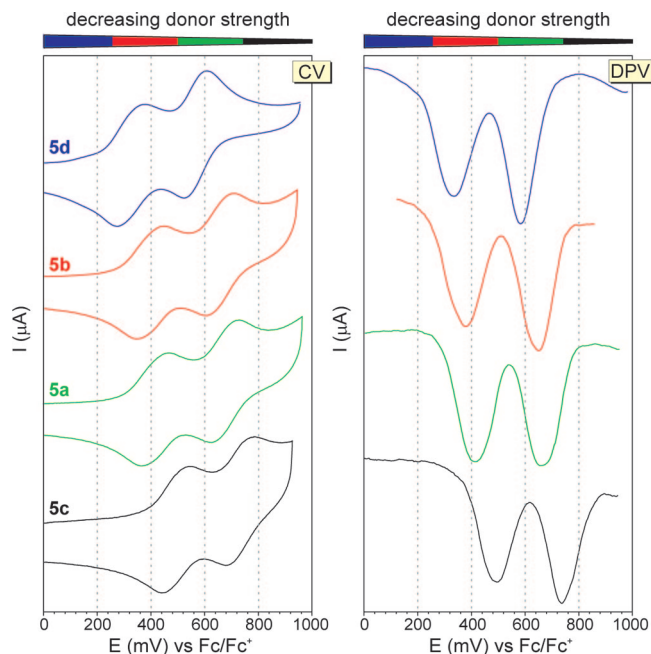
The versatile synthetic route to the novel class of 'superbiaryls' as presented in this paper permits free variation of the central metals, thus paving the way to selectively tune the rotational barrier of these porphyrin-derived 'superbiaryls' and permitting the design of bimetal systems with defined rotational stability at the biaryl axis.

Cyclovoltammetric Studies. For an investigation of the oxidation properties of all metalated and nonmetalated bisporphyrins, *rac*-**4a**−**4i** and *rac*-**5a**−**5i**, cyclic voltammograms (CVs) in CH$_2$Cl$_2$/tetrabutylammonium hexafluorophosphate (TBAH) solution (Table 7) were measured. All bisporphyrins showed at least two oxidation waves which were assigned to four oxidation processes: (a) P−P → P$^+$−P, (b) P$^+$−P → P$^+$−P$^+$, (c) P$^+$−P$^+$ → P^{2+}−P$^+$, (d) P^{2+}−P$^+$ → P^{2+}−P^{2+}. In most cases, processes (a) and (b), as well as processes (c) and (d), were found to be covered by one unresolved wave. For a more accurate determination of the separation between the redox potentials of the first and second oxidation steps (processes (a)

Figure 12. CVs (scan rate: 250 mV s^{-1}) and DPVs of **5d**, **5b**, **5a**, **5c** with decreasing donor strength of the meso substituents in this order.

and (b), see above), differential pulse voltammetry (DPV) was performed. Table 7 shows the determined redox potentials and ΔE values.

The oxidation potentials of the porphyrins are known to be influenced by two effects: the donor strength of the meso substituents and the electronic character of metal ion. As expected, the oxidation potentials of both, the metalated and the free-base porphyrins increased with decreasing donor strength of the meso substituents, viz. **4d** < **4b** < **4a** < **4c** and **5d** < **5b** < **5a** < **5c** (Table 7). As an example, the CVs and DPVs of zincated compounds *rac*-**5a**−**5d** are shown in Figure 12.

Furthermore, even the *type* of metal was found to influence the oxidation potentials of the bisporphyrins significantly. As indicated by the data in Table 7, the oxidation potentials increased in the order zinc(II) < copper(II) < free-base < nickel(II) < palladium(II) for porphyrins *rac*-**5a**, *rac*-**5f**, *rac*-**4a**, *rac*-**5g**, and *rac*-**5i** with identical meso substituents. Another effect that occurred upon exchange of the metal ion, was a variation of the potential splitting (ΔE) between the first oxidation step and the second one. All zinc(II) bisporphyrins showed a single wave for the first two oxidation processes, which was not resolvable even by DPV like, e.g., *rac*-**5a** in Figure 12. For the copper(II), nickel(II), and palladium(II) derivatives and for the free-base bisporphyrin *rac*-**4a**, by contrast, well separated waves were observed at least in the DPV measurements (see, e.g., CV and DPV of *rac*-**5g** in Figure 13).[67]

Conclusion

A series of novel, directly β,β'-linked—and thus intrinsically axially chiral—bisporphyrins have been synthesized. The preparation involved a Pd-catalyzed Miyaura-like transmetalation of monobrominated porphyrins. This reaction, which is unprecedented in porphyrin chemistry with respect to the sterical requirements at the coupling position, necessitated the development of a method for the formation of a variety of novel β-boronic acid esters of tetraarylporphyrins. Our optimized
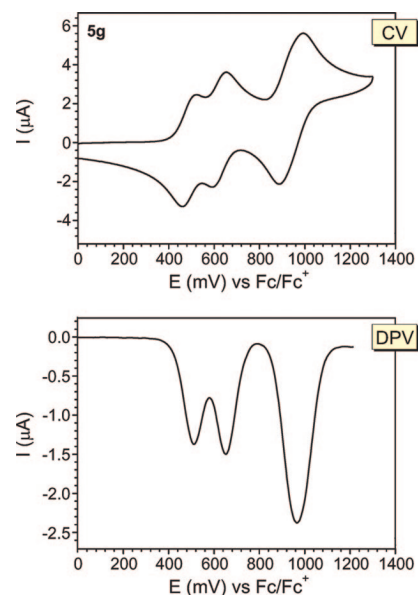
Figure 13. CV (top) and DPV (bottom) of *rac*-**5g** in 0.1 M TBAH in CH$_2$Cl$_2$ referenced vs Fc/Fc$^+$ as the internal standard. The first two oxidation processes are clearly split.

reaction conditions now open up an efficient access to β-borylated porphyrins with four meso-aryl substituents. These as yet unknown porphyrin derivatives should be of high synthetic value, not only in terms of the construction of bisporphyrins described in this paper, but also as versatile building blocks for the design of diverse β-functionalized porphyrins[46] and large porphyrin assemblies.[32]

The key step of the synthesis was a Suzuki coupling of the boronic acid esters **3a**−**k** with the brominated porphyrins **1a**−**k**. By application of the optimized procedure, various novel β,β'-bisporphyrins have become available in good yields differing in their substitution pattern and in their metalation state. The coupling step is highly efficient and variable, which was demonstrated by the directed synthesis of unsymmetric bisporphyrins either bearing different meso-aryl residues in the porphyrin moieties (like *rac*-**4e** and *rac*-**5e**) or two different metal centers (*rac*-**4g**−**i**), and by the preparation of monometalated representatives, as exemplarily shown by the synthesis of *rac*-**4f**.

In their metalated form, most of the novel-type bisporphyrins thus prepared were shown to be rotationally stable and thus axially chiral and were fully characterized stereochemically by stopped-flow HPLC-CD experiments assisted by quantum chemical CD calculations. The barrier of rotation about the chiral porphyrin-porphyrin axis was found to be strongly dependent on the nature of the metal centers coordinated by the bispor-

(67) It is tempting to interpret this potential splitting as being due to different electronic 'communication' between the two porphyrin subunits, also because many other factors like, e.g., ion pairing effects, control the redox splitting significantly.[68] On the other hand, Arnold et al.[69] observed an analogous behavior for butadiyne-bridged metalated octaethyl-substituted bis(octaethylporphyrins) and attributed this wave splitting to aggregate formation of cationic porphyrin units.[70] Despite the apparent steric hindrance by the meso substituents it might indeed be imaginable that the meso-aryl substituted bisporphyrins in this paper may form aggregates.
(68) Barrière, F.; Geiger, W. E. *J. Am. Chem. Soc.* **2006**, *128*, 3980–3989.
(69) Arnold, D. P.; Heath, G. A.; James, D. A. *J. Porphyrins Phthalocyanines* **1999**, *3*, 5–31.
(70) Brancato-Buentello, K. E.; Kang, S.-J.; Scheidt, W. R. *J. Am. Chem. Soc.* **1997**, *119*, 2839–2846.

phyrin backbone, thus offering the opportunity to selectively manipulate the chiroptical properties of these novel 'superbiaryls'. Such a phenomenon or a similar metal influence on the atropisomerization process of bisporphyrins has not been described so far.

This previously not observed tuning of a chiral porphyrin−porphyrin axis by variation of the central metals in the porphyrin subunits was additionally confirmed and further rationalized by quantum chemical calculations with the BLYP-D method. Using the dispersion correction, which turned out to be a substantial improvement for the calculations on the porphyrin dimers, the computational investigations showed that the ring strain of the monomeric porphyrin subunits as a consequence of the presence and type of the central metals is decisive for the rotational barrier. Whereas zinc(II), palladium(II), and copper(II) fit quite well into the porphyrin ring and therefore result in planar subunits, nickel(II) tends to be tetrahedrally coordinated in the ground state, leading to a ruffled conformation of the nickelated porphyrin moieties and to a significantly different structure of the transition state in comparison to those of the other metalated bisporphyrins and, thus, to a much lower rotational barrier.

In contrast to directly linked chiral bis-TAPs reported previously,[30] the axial chirality of these extended biaryls is independent from the substitution pattern of the porphyrin backbone,[29] which permits a more convenient preparation, without any restrictions concerning the symmetry of the monomeric substructures. The described bisporphyrins open a vast, stereochemically largely differentiated cavity including two freely combinable metal centers, giving rise to promising applications of such compounds as mono- or bimetallic catalysts in asymmetric synthesis or as chiral reporter groups. Moreover, β,β′-bisporphyrins might open new perspectives for the design of optical and electronic devices, and of novel materials with unique chiral and chiroptical properties. These expected properties and possible applications make the development of a first directed access to enantiopure material by the atropo-enantioselective synthesis of axially chiral porphyrin-derived compounds a rewarding task. This work is in progress.

Experimental Section

Synthesis of β-Borylated Tetraarylporphyrins 3 (Typical Procedure): 2-(4′,4′,5′,5′-Tetramethyl-[1′,3′,2′]dioxaborolan-2′-yl)-5,10,15,20-tetraphenylporphyrin (3a). Under a nitrogen atmosphere, a suspension of 2-bromo-5,10,15,20-tetraphenylporphyrin (**1a**, 558 mg, 804 μmol, 1 equiv), KOAc (790 mg, 8.04 mmol, 10 equiv), and 4,4,5,5-tetramethyl-2-(4′,4′,5′,5′-tetramethyl-[1′,3′,2′]-dioxaborolan-2-yl)-[1,3,2]dioxaborolane (510 mg, 2.02 mmol, 2.5 equiv) in toluene (200 mL) and deionized H_2O (40 mL) was degassed with nitrogen in an ultrasonic bath for 15 min. Pd(dppf)Cl$_2$ (131 mg, 161 μmol, 20 mol %) was added and the reaction mixture was heated to 110 °C for 3 h with vigorous stirring. After addition of CH_2Cl_2 to the suspension, the organic phase was washed with H_2O and saturated aqueous NH_4Cl. The combined organic layers were dried over $MgSO_4$, the solvent was removed in vacuo, and the resulting solid was purified by column chromatography on silica gel using petroleum ether/CH_2Cl_2 (5:1 to 0:1, v/v) as the eluent to yield **3a** as a purple solid (414 mg, 558 μmol, 70%). mp (CH$_2$Cl$_2$/MeOH) > 300 °C; IR (KBr): $\tilde{\nu}$ = 3450 (w), 2976 (m), 2853 (w),

1474 (m), 1349 (m), 1141 (s), 1029 (s), 964 (m), 800 (m) cm^{-1}; ^{1}H (400 MHz, CDCl$_3$): δ −2.64 (s, 2H, NH), 1.20 (s, 12H, pinacol), 7.67−7.85 (m, 12H, *m/p*-Ar-H), 8.15−8.31 (m, 8H, *o*-Ar-H), 8.65 (d, J = 4.8 Hz, 1H, β-pyrrole-H), 8.74 (d, J = 4.8 Hz, 1H, β-pyrrole-H), 8.78−8.86 (m, 4H, β-pyrrole-H), 9.14 (s, 1H, β-pyrrole-H); ^{13}C NMR (100 MHz, CDCl$_3$): δ 25.6, 84.1, 127.0, 127.1, 128.0, 128.1, 134.9, 135.0, 135.2, 136.6, 161.0; MS (EI, 70 eV): *m/z* (%) = 740 (100) [M$^+$], 613 (15) [M$^+$ − BPin]; HRMS (ESI) calcd for C$_{50}$H$_{42}$BN$_4$O$_2$ [M + H$^+$] 741.3401, found 741.3401; UV−vis (CH$_2$Cl$_2$): λ_{max} (log ε) = 421 (5.56), 519 (4.20), 555 (3.86), 596 (3.71), 656 (3.74) nm; Anal. Calcd for C$_{50}$H$_{41}$BN$_4$O$_2$: C, 81.08; H, 5.58; N, 7.56; found: C, 81.62; H, 5.65; N, 7.60.

Synthesis of β,β′-Bisporphyrins 4 (Typical Procedure): β,β′-Bis(5,10,15,20-tetraphenyl-porphyrin) (*rac*-4a). A Schlenck flask filled with boronic ester **3a** (300 mg, 406 μmol, 1 equiv), 2-bromo-5,10,15,20-tetraphenylporphyrin (**1a**, 338 mg, 488 μmol, 1.2 equiv), and Ba(OH)$_2$·8H$_2$O (1.28 g, 4.06 mmol, 10 equiv) was evacuated and flushed with nitrogen three times. Toluene (160 mL) and deionized H_2O (32 mL) were added and the solution was degassed by a nitrogen stream in an ultrasonic bath for 15 min. Pd(PPh$_3$)$_4$ (93.8 mg, 81.2 μmol, 20 mol %) was added and the resulting mixture was refluxed for 14 h with vigorous stirring. After addition of H_2O and CH_2Cl_2, the organic phase was separated and the aqueous layer was extracted three times with CH_2Cl_2. The combined organic layers were washed with H_2O and saturated aqueous NH_4Cl and dried over $MgSO_4$. Concentration of the filtrate and purification of the resulting residue by column chromatography on silica gel using petroleum ether/CH_2Cl_2 (4:1 to 0:1, v/v) as the eluent afforded *rac*-**4a** as a purple solid (364 mg, 296 μmol, 73%). mp (CH$_2$Cl$_2$/MeOH) > 300 °C; IR (KBr): $\tilde{\nu}$ = 3439 (w), 2921 (m), 1616 (w), 1511 (m), 1461 (m), 1020 (m), 964 (m), 795 (s) cm^{-1}; ^{1}H (400 MHz, CDCl$_3$): δ −2.71 (bs, 2H, NH), 3.98 (bs, 1H, Ar−H), 4.92 (bs, 1H, Ar−H), 6.34 (bs, 1H, Ar−H), 6.57 (d, J = 6.7 Hz, 1H, Ar−H), 7.30 (d, J = 7.4 Hz, 1H, Ar−H), 7.62−7.88 (m, 9H, Ar−H), 8.02 (d, J = 4.8 Hz, 1H, β-pyrrole-H), 8.10 (bs, 1H Ar−H), 8.17−8.29 (m, 3H, Ar−H), 8.36−8.46 (m, 2H, Ar−H), 8.54 (d, J = 4.8 Hz, 1H, β-pyrrole-H), 8.73 (s, 1H, β-pyrrole-H), 8.82 (d, J = 4.8 Hz, 1H, β-pyrrole-H), 8.85−8.88 (m, 2H, β-pyrrole-H), 8.90 (d, J = 4.8 Hz, 1H, β-pyrrole-H); ^{13}C NMR (100 MHz, CDCl$_3$): δ 45.9, 119.8, 119.9, 120.0, 120.3, 123.2, 124.4, 124.9, 126.6, 126.8, 127.6, 127.7, 127.8, 130.7, 134.5, 134.6, 135.0, 139.8, 142.2, 142.4, 142.7, 145.2; HRMS (ESI) calcd for C$_{88}$H$_{59}$N$_8$ [M + H$^+$] 1227.4857, found 1227.4869; UV−vis (CH$_2$Cl$_2$): λ_{max} (log ε) = 423 (5.55), 438 (5.54), 523 (4.64), 555 (4.15), 596 (4.10), 652 (3.74) nm.

Supporting Information Available: General experimental details, complete experimental procedures, copies of the ^{1}H spectra, CD spectra, chromatographic conditions for the resolution of the atropo-enantiomers, data of the kinetic study of the atropo-enantiomerization, UV data, information concerning the computational methods, and details of the crystal structure determination. This material is available free of charge via the Internet at http://pubs.acs.org.

JA8055886